Quaternary Science Reviews 344 (2024) 108972

Contents lists available at ScienceDirect

Quaternary Science Reviews

journal homepage: www.elsevier.com/locate/quascirev

The last glacial cycle in southernmost Patagonia: A review

Carla Huynh [a,*], Andrew S. Hein [a], Robert D. McCulloch [a,b], Robert G. Bingham [a]

[a] School of GeoSciences, University of Edinburgh, UK
[b] Centro de Investigación en Ecosistemas de la Patagonia (CIEP), Coyhaique, Chile

ARTICLE INFO

Handling editor: C. O'Cofaigh

Keywords:
Glacial chronology
Last glacial maximum
Glacial geomorphology
Patagonian ice sheet
South America
Radiocarbon dating
Cosmogenic nuclide exposure dating
Empirical reconstruction
Palaeoclimate

ABSTRACT

This paper systematically reviews the geomorphological and geochronological evidence of the last glacial cycle (~115-11.7 ka) south of 52°S in southernmost Patagonia. We review the extent and timing of glaciation, compile geochronometric data from published studies into an open-access database and present an updated empirical reconstruction of ice-sheet evolution. The extent and timing of the local Last Glacial Maximum is ambiguous and we review the data that indicate that the local Last Glacial Maximum occurred during Marine Isotope Stage (MIS) 3/MIS 4 versus during MIS 2 at the time of the global Last Glacial Maximum. These contrasting scenarios differ by ~100 km in lateral ice extent and 10s of thousands of years in timing, implying drastically different past environmental conditions, and therefore drivers. All of the major ice lobes were extensive until at least 18 ka and the onset of deglaciation occurred at ~18-17 ka. The southernmost Patagonian Ice Sheet rapidly collapsed to the Fuegian fjords in <1000 years, likely due to the lower altitude of the Andes in this region, lower slopes of the glacier surfaces and through ice calving within the deep fjords into which the ice sheet retreated. During the Antarctic Cold Reversal (~14.7-13 ka), glaciers readvanced only a few kilometres, restricted to the Fuegian fjords, and not ~100 km to a 'Stage E' moraine, as previously hypothesised. This review highlights the disparity of dating constraints across southernmost Patagonia and suggests possible approaches for further study. More work is required to understand and resolve the discrepancy in the geochronological data and to determine a robust empirical reconstruction for the maximum last glacial extent in southernmost Patagonia, which is imperative for making climate inferences and comparing to numerical ice-sheet models.

1. Introduction

Reconstructing the timing and extent of glaciation and deglaciation provides an important line of evidence for reconstructing the variability of past climate fluctuations across the Earth. Patagonia offers unique insight into past climate because it is the only continental landmass, and hence ice-sheet nucleation centre, that extends sufficiently far south from the midlatitudes to intercept the Southern Westerly Winds (SWWs), changes to which are influential in driving fluctuations in global ocean circulation (Moreno et al., 2018). Landforms associated with the last glacial cycle in Patagonia (~115-11.7 ka) are well preserved, and record that at its maximum the Patagonian Ice Sheet (PIS) extended ~1800 km from north to south along the southern Andes Mountain Range, covering ~17° of latitude and containing ~492,600 km^2 of ice (Davies et al., 2020; Rabassa et al., 2022). The PATICE reconstruction summarised our current knowledge of PIS evolution from 35 ka to the present by compiling published glacial chronologies across the entire ice sheet between 38°S and 55°S for 5000-year intervals (Davies et al., 2020). However, this reconstruction of the timing and extent of glaciation in southernmost Patagonia is based on a partial set of evidence. Across this region, there are discrepancies in the published geochronology that lead to contradictory interpretations of the local Last Glacial Maximum (lLGM) that differ by ~100 km in lateral extent and ~10,000 years in timing (Darvill et al., 2015b; McCulloch et al., 2005a), and there is moreover paradoxical evidence for either a rapid and substantial deglaciation before 17 ka (Hall et al., 2019) or a significantly more extensive glaciation until 12 ka (McCulloch et al., 2005b). Explaining and reconciling these contrasting interpretations is vital to better constrain our knowledge of past climate fluctuations in the region and thus better understand its impacts upon and integration with wider global atmospheric and oceanic circulation. This, in turn, has motivated us here to compile a more in-depth review of the timing and extent of glaciation across southernmost Patagonia since the lLGM incorporating data that have been published since the PATICE reconstruction was produced.

Firstly, we review in turn the geomorphological and

* Corresponding author.
E-mail address: carla.huynh@ed.ac.uk (C. Huynh).

https://doi.org/10.1016/j.quascirev.2024.108972
Received 2 May 2024; Received in revised form 6 September 2024; Accepted 12 September 2024
Available online 25 September 2024

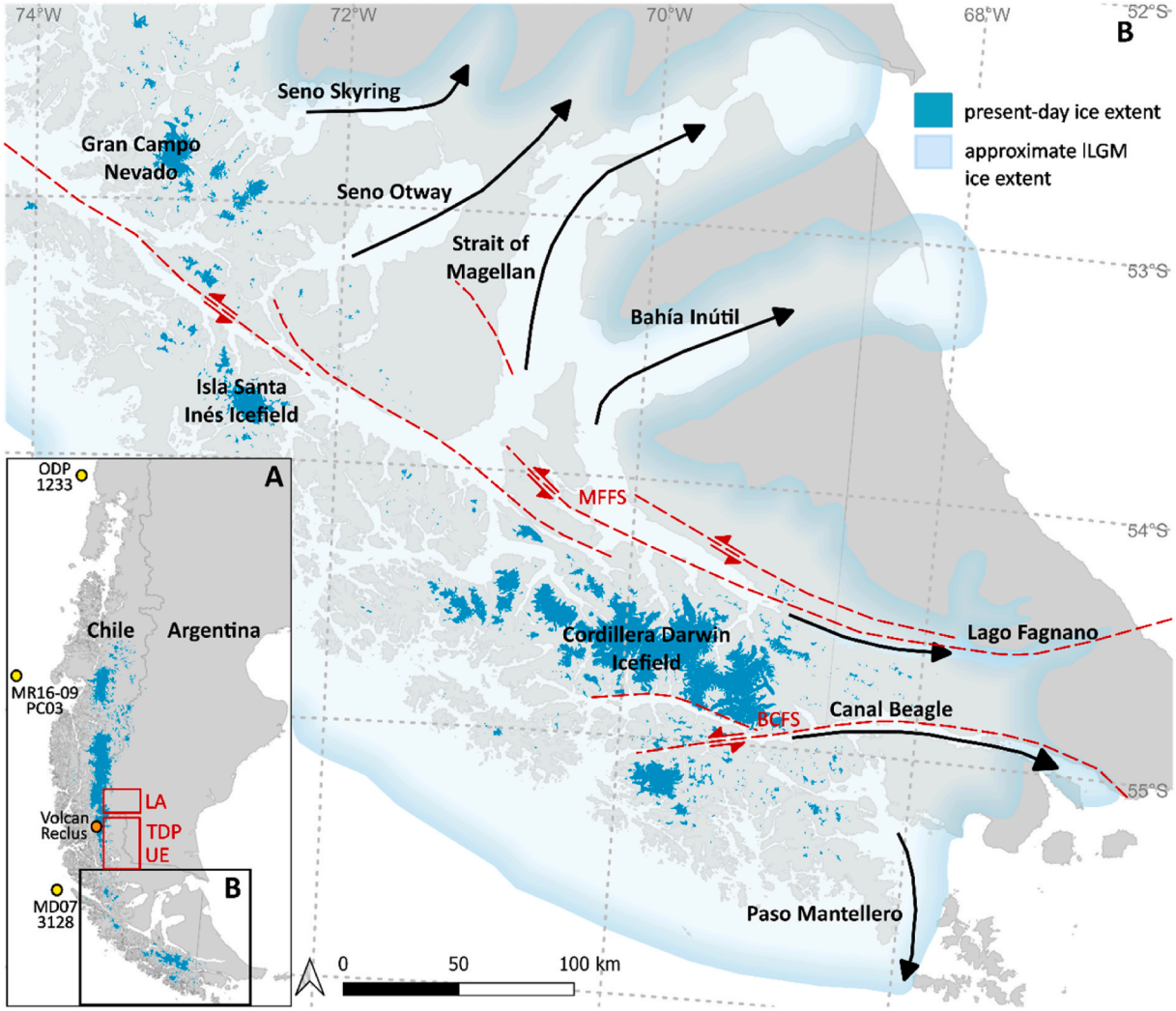

Fig. 1. (A) Location of the study area in Patagonia. The red boxes show the positions of Lago Argentino (LA), Torres del Paine (TDP) and Última Esperanza (UE) ice lobes immediately north of the study area, yellow circles are the locations of marine sediment cores (S–N: Caniupán et al., 2011; Hagemann et al., 2024; Kaiser et al., 2007) and the orange circle is the Reclus volcano. (B) Stylised representation of the southernmost part of the former PIS, highlighting the ice lobes mentioned in the text (approximate lLGM extent adapted from Darvill et al. (2015b, 2017), Coronato et al. (2009), Rabassa et al. (2006) and Hodgson et al. (2023) for Seno Skyring and Seno Otway, Strait of Magellan and Bahía Inútil, Lago Fagnano, Canal Beagle and Paso Mantellero ice lobes respectively). Present-day ice shapefiles indicated in dark blue are from the Randolph Glacier Inventory (RGI 7.0 Consortium, 2023). The Magellan-Fagnano Fault System (MFFS) and Beagle Channel Fault System (BCFS) indicated in red are from Betka et al. (2016) and Sandoval and De Pascale (2020).

geochronometric evidence of the last glaciation for the PIS's southernmost ice lobes (from north to south: Seno Skyring, Seno Otway, Strait of Magellan, Bahía Inútil, Lago Fagnano, Canal Beagle, Paso Mantellero; Fig. 1), with particular emphasis on moraine chronology, which provides direct evidence of ice-lobe stabilisation. For each ice lobe, we recalculate and recalibrate the available chronological data to ensure consistency between studies and reflect the most recent advances in the calculation of radiocarbon and cosmogenic ^{10}Be ages (Heaton et al., 2020; Hogg et al., 2020; Kaplan et al., 2011; Lifton et al., 2014) and we present possible Gaussian distributions for constraining the ages of moraine deposition. We review in detail the regions that are characterised by conflicting observations in the literature and, in doing so, we highlight knowledge gaps where future research could be focused and provide the context and caveats from which empirical reconstructions and climate inferences can be made.

2. Background and methods

2.1. Geographic setting

We focus on the southernmost part of Patagonia: The South American mainland south of ~52°S, the Strait of Magellan and the Fuegian archipelago. The region is bisected by a continental transform fault (the Magellan-Fagnano Fault System; Fig. 1) demarking the boundary between the South American Plate to the north and the Scotia Plate to the south (Ammirati et al., 2020). Here, the N-S trending Andes mountain range curves eastward and lowers in elevation and several small icefields and glaciers are the remnants of the former PIS (Fig. 1). The elevation of these icefields is considerably lower than the Andes further north, with maximum altitudes of 1740 m a.s.l. (Monte Pyrámide; Schneider et al., 2007), 1399 m a.s.l. (unnamed peak; Gurdiel et al., 2022) and 2469 m a.s.l. (Mount Darwin; Holmlund and Fuenzalida, 1995) in the Gran Campo Nevado, Isla Santa Inés and Cordillera Darwin Icefields, respectively.

Southernmost Patagonia is the only continuous continental landmass that intersects the core of the SWWs, which are currently positioned

between ~50 and 55°S (Lamy et al., 2010). The regional climate is strongly controlled by the position and strength of the SWWs, which flow west to east across the southern tip of South America (Garreaud et al., 2013). The Andes mountain chain forms a topographic barrier perpendicular to their flow resulting in a strong west-east precipitation gradient due to the orographic uplift of humid air masses from the Pacific Ocean. This results in an enhanced rain shadow in the lee of the Andes, leading to arid conditions and an average annual rainfall of ~400 mm on the eastern side, compared to ~4000 mm in the west (Fick and Hijmans, 2017).

2.2. Methods

We present a combined and simplified schematic of the published geomorphological mapping pertaining to the last glacial cycle for the southernmost PIS ice lobes (Bentley et al., 2005; Coronato et al., 2009; Darvill et al., 2014; Davies et al., 2020; Glasser and Jansson, 2008; Hodgson et al., 2023; Lira et al., 2022; Lovell et al., 2012; Soteres et al., 2020). We define 'moraine limits' as digitised lines drawn at the maximum extent of mapped moraines relating to that glacial stage. Whilst we recognise that simplifying comprehensive geomorphological mapping from multiple publications to a single simplified framework of glaciation across multiple glacial valleys has its limitations and needs to be interpreted with due caution, it represents a helpful initial exercise for comparing the timing and extent of glaciation across the region.

We review the literature and compile published radiocarbon and cosmogenic ^{10}Be ages that are associated with these mapped moraines following the methods of Davies et al. (2020; the PATICE database). Our compilation represents a significant update to the 2020 PATICE database, incorporating 103 newly published cosmogenic ^{10}Be ages and 13 new radiocarbon ages from recent studies in southernmost Patagonia. The moraine to which each date is assigned was determined by the geomorphological link to that limit as defined by the original field study. Where specific coordinate data were omitted in the original study, we

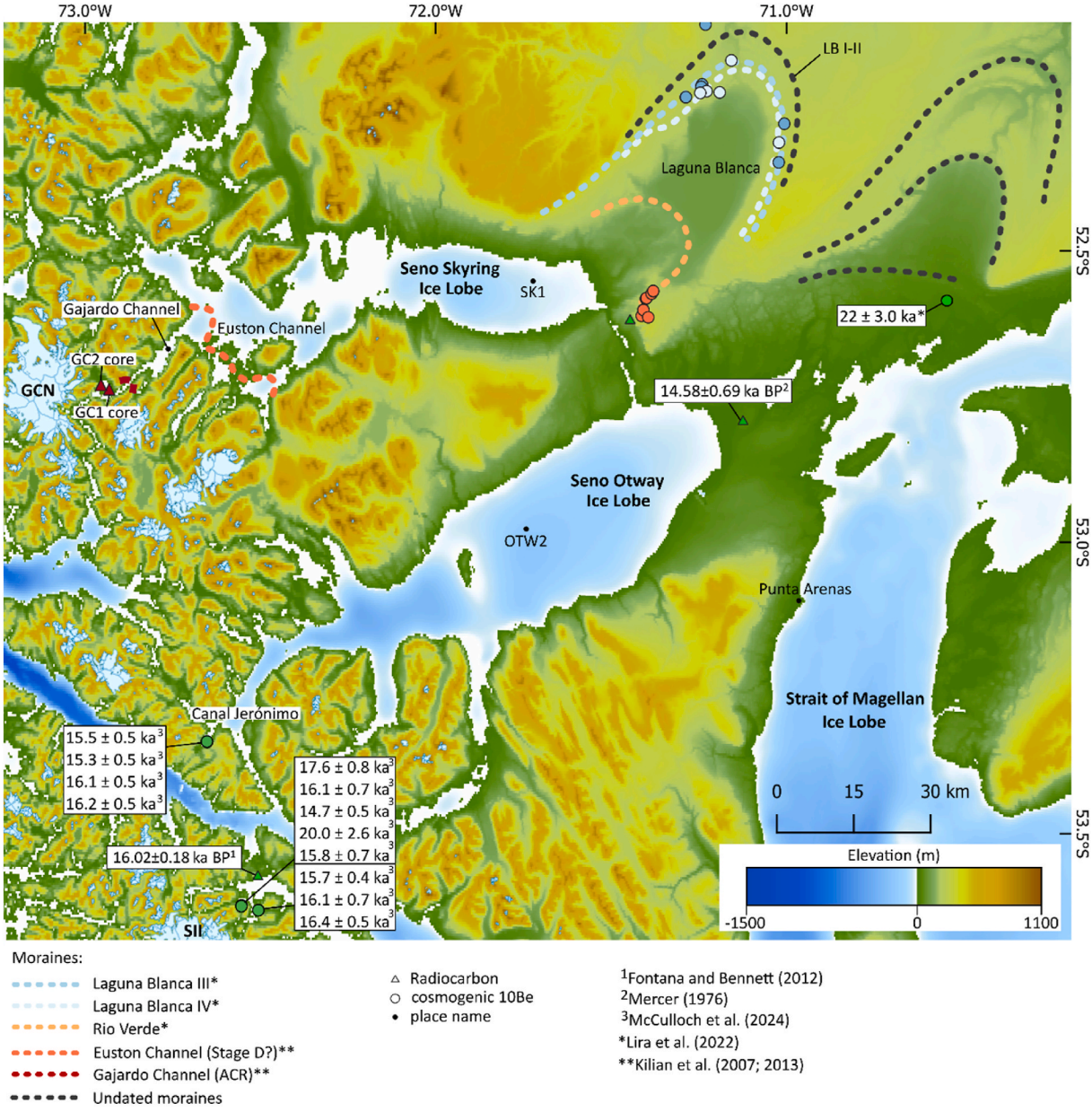

Fig. 2. The locations of previously mapped moraine limits and geochronometric dating sites for Seno Skyring and Seno Otway ice lobes, displayed on the ETOPO 2022 15 Arc-Second Global Relief Model. See Fig. 6 and the supplementary data for recalculated ages. GCN = Gran Campo Nevado; SII = Santa Inés Icefield.

estimate the locations of reported dates from the location map in the original study.

We recalibrate/recalculate radiocarbon and cosmogenic ^{10}Be ages from existing studies to reflect the most recent advances in the radiocarbon calibration curve and cosmogenic ^{10}Be production rate and scaling scheme and ensure that consistent corrections are applied to the whole dataset. All recalculated ages are available in the supplementary data. Reported dates throughout this paper refer to ages recalculated in this study, and hence may differ slightly from the original study. Where we report weighted arithmetic means, we determined these from the recalculated ages in this study. We recalculated cosmogenic ^{10}Be ages using the online calculator formerly known as the CRONUS-Earth online calculator version 3 (Balco et al., 2008) using the LSDn scaling scheme (Lifton et al., 2014), the local ^{10}Be production rate for southern Patagonia (Kaplan et al., 2011) and assuming no rock surface erosion or surface shielding (e.g., by snow, soil, etc). We recalibrated radiocarbon ages against the SHCal20 calibration curve for terrestrial samples (Hogg et al., 2020) and the Marine20 curve for marine samples (Heaton et al., 2020) using OxCal online Version 4.4 (Bronk Ramsey, 2009).

Here, we report recalculated cosmogenic ^{10}Be ages to one decimal place with the unit 'ka', meaning thousands of years before the sampling date. In the text we report the 1σ internal (analytical) uncertainty to facilitate comparisons between cosmogenic nuclide data. The full external uncertainty is available in the supplementary data. We report recalibrated radiocarbon ages to two decimal places alongside the 2σ error; this represents a ~95% probability of the calibrated date falling within this range. The unit 'cal ka BP' is used for calibrated radiocarbon dates, with 'BP' meaning years before 1950 AD.

Overall, we compiled 196 cosmogenic ^{10}Be dates and 129 radiocarbon dates from existing publications. Fourteen cosmogenic ^{10}Be dates were not reported with associated AMS measurements precluding us from recalculating them. Similarly, four radiocarbon dates were not originally reported alongside uncalibrated radiocarbon ages and so are not recalibrated. These non-recalculated ages are indicated in the text with an asterisk. Seven of the radiocarbon ages are infinite radiocarbon ages. Thus, there are 182 recalculated cosmogenic ^{10}Be dates and 118 non-infinite recalibrated radiocarbon dates.

Interpreting datasets of cosmogenic ^{10}Be ages, particularly where age distributions are skewed or poorly clustered, is challenging, as there are many factors that can lead to anomalously young or old cosmogenic ^{10}Be ages. Under ideal assumptions, a boulder sampled from a moraine crest experienced no prior exposure before deposition and has since been continuously exposed. However, if prior exposure is not completely eroded away during transport (nuclide inheritance) or the sample experiences post-depositional processes (e.g., rolling, shielding, exhumation or erosion) the resulting cosmogenic ^{10}Be age will overestimate or underestimate the true age of the moraine, respectively (Balco, 2020; Heyman et al., 2011; Hein et al., 2014). This is further compounded by the often-small sample sizes of cosmogenic ^{10}Be ages (due to limited suitable sample material and the expense of cosmogenic ^{10}Be dating), which make the data extremely sensitive to the choice of statistical test (Applegate et al., 2010, 2012; Balco, 2011; Dortch et al., 2022).

Since some of the published cosmogenic ^{10}Be ages for moraines in southernmost Patagonia exhibit considerable geological scatter, we present all recalculated ages and uncertainties, with no outliers removed, and use the Probabilistic Cosmogenic Age Analysis Tool (P-CAAT Version 2.2; Dortch et al., 2022) to suggest Gaussian distributions that could represent the timing of moraine deposition based on the distribution of available data. P-CAAT is a new statistical approach for cosmogenic ^{10}Be age outlier detection and landform-age analysis which generates a Probability Density Estimate (PDE) based on input ages and performs Gaussian separation of the PDE using a Monte Carlo-style approach. A choice of three bandwidth estimators is available within the programme to generate the model fit: mean, Standard Deviation/Inter-quartile Range (STD/IQR) and Mean Absolute Dortch Deviants (MADD). Selecting the most suitable bandwidth estimator is important, so that the model does not under or overfit the data. We select the most suitable bandwidth for each moraine dataset using the three insight plots and r-squared value, following the method recommended by Dortch et al. (2022). We present all individual mean exposure ages and internal uncertainties, along with the component Gaussians derived using the selected bandwidth estimator, to demonstrate the range of possible interpretations of the moraine age. For further explanation of the P-CAAT programme, see Dortch et al. (2022) and for a list of selected bandwidth estimators see the supplementary data.

To avoid making potentially invalid assumptions, the datasets of cosmogenic ^{10}Be ages from the Strait of Magellan and Bahía Inútil ice lobes are considered independently. Moraine limits of the two lobes have been correlated in the literature, but the geomorphology of the area around Cabo Boquerón, where the two ice lobes diverge, has not been comprehensively mapped to date.

We then combine the recalculated geochronometric dates and geomorphological evidence with topographic and bathymetric data (ETOPO, 2022) in QGIS and use these alongside the P-CAAT analysis and literature review to inform an updated ice-sheet reconstruction of the southernmost PIS. Shapefiles of each timeslice are available in the supplementary data.

3. Seno Skyring Ice Lobe

Seno Skyring Ice Lobe extended ~150 km from present-day Gran Campo Nevado (GCN) during the last glacial cycle (Figs. 1 and 2). The ice lobe flowed northeast through fjords surrounding the GCN, eastwards through the ice-scoured trough occupied by Seno Skyring and terminated on the northern shore of Laguna Blanca (Kilian et al., 2007b; Lira et al., 2022, Fig. 2). GCN, which during full glacial conditions was connected to the PIS, sits at a lower elevation than Cordillera Darwin Icefield (CDI) and the Southern Patagonian Icefield and, based on field observations, the slope of the glacier surface during the LGM was very low (<5‰; Kilian et al., 2007a). This would have made Seno Skyring Ice Lobe very sensitive to changes in equilibrium line altitude and hence small-scale climate changes during the last glacial termination could have resulted in large changes to the glacier mass balance (Kilian et al., 2007a).

Lira et al. (2022) proposed a chronology for the last glacial extent of Seno Skyring Ice Lobe. Two moraine systems were identified: the outer Laguna Blanca (LB), which is comprised of four limits named, from oldest to youngest, LB I-IV, and the inner Río Verde (RV) moraine (Fig. 2). Cosmogenic ^{10}Be dating of moraine boulders suggests that the LB III and LB IV moraines formed at 25.8 ± 2.5 ka (n = 5) and 23.7 ± 0.9 ka (n = 3) respectively. Although the most extensive LB I and LB II moraines remain undated, because of the absence of datable moraine boulders, Lira et al. (2022) suggested relatively contemporaneous formation of the whole Laguna Blanca moraine system due to it comprising similar morphostratigraphic characteristics throughout the whole system. The inference is that the lLGM of Seno Skyring Ice Lobe was attained during the gLGM (~26.5-19 ka; Clark et al., 2009). However, Lira et al. (2022) consider that the single boulder with an age of 40.0 ± 6.1 ka deposited on the LB III moraine could signify that the glacier was at or close to the LB position during an earlier MIS 3 advance (MIS 3–29–57 ka; Lisiecki and Raymo, 2005), in keeping with the glacial chronologies from Última Esperanza and Torres del Paine ice lobes to the north (García et al., 2018; Sagredo et al., 2011). Alternatively, this statistical outlier may simply contain inherited ^{10}Be from a previous exposure. The inner RV moraine exhibits distinctly sharper slopes and higher relief compared to the LB moraine system and cosmogenic ^{10}Be dating on this moraine yielded an age of 18.1 ± 1.4 ka (n = 6). Based on a minimum-limiting radiocarbon age from basal peat inboard of the RV moraine, retreat from this moraine limit had occurred by at least 16.40 ± 0.17 cal ka BP (Lira et al., 2022).

A 4.7 m sediment core was retrieved from eastern Seno Skyring (SK1;

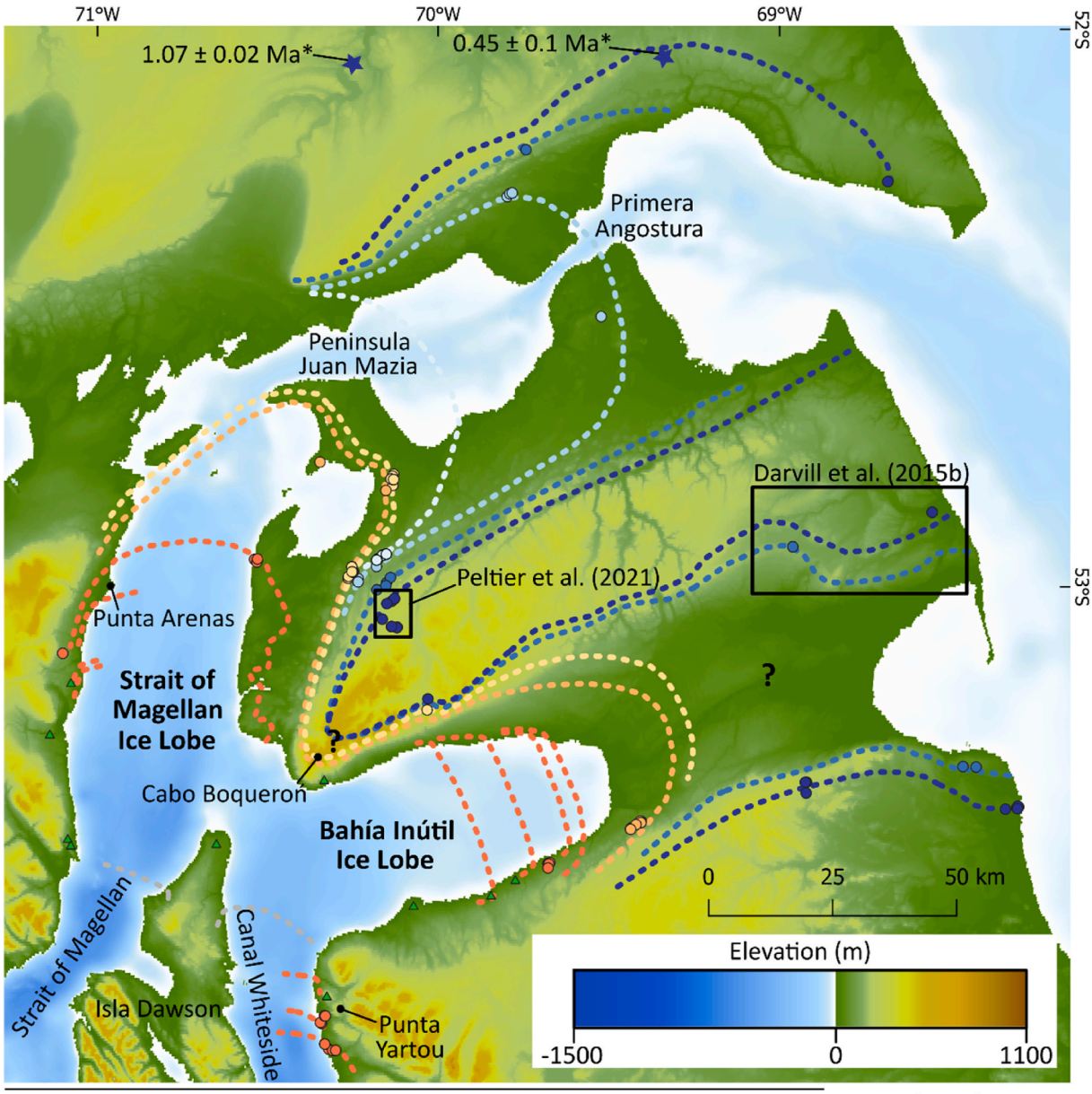

	Strait of Magellan moraine name	Bahía Inútil moraine name
	Cabo Vírgenes	**Río Cullen**
	Punta Delgada	**Sierras de San Sebastián**
	Primera Angostura	Lagunas Secas
	Stage A	-
	Segunda Angostura (**Stage B**)	**Stage B**
	Stage C	**Stage C**
	Stage D	**Stage D**
	Previously hypothesised 'Stage E' ice dam	

△ Radiocarbon
○ Cosmogenic 10Be
☆ 40Ar/39Ar
• place name

*Meglioli (1992)

Fig. 3. The approximate locations of previously mapped moraine limits and the corresponding limit names for Strait of Magellan and Bahía Inútil ice lobes, displayed on the ETOPO 2022 15 Arc-Second Global Relief Model. For clarity, the moraine-limit names in bold are used to refer to the equivalent limit in both ice lobes throughout this paper. The location of radiocarbon and cosmogenic ^{10}Be sample sites are also shown. See the supplementary data for recalculated ages and references. The "?"indicates the uncertain correlation of the PA and Stage A moraines in the central depression of Bahía Inútil Ice Lobe due to subdued and discontinuous hummocky moraine (Darvill et al., 2017). Locations of sample sites that provide evidence for a more extensive and earlier lLGM during MIS 3 (Darvill et al., 2015b) and MIS 4 (Peltier et al., 2021) are indicated with black boxes.

Fig. 2) in 72 m water depth by Kilian et al. (2007a). In this, an ice-rafted debris (IRD) layer was found beneath a layer of the robustly-dated Volcan Reclus tephra (15.0 ka; Sagredo et al., 2011; McCulloch et al., 2005b). From estimating the sedimentation rate, the IRD layer was suggested to have been formed between 17.46 and 18.28 ka BP*, suggesting that Seno Skyring Ice Lobe was in retreat from the RV moraine limit at this time. The SK1 core also contains a relatively high clay fraction and MgO content between ~16-13.5 ka BP*. This is thought to be indicative of chlorine-rich sediment transport from the mafic lithologies of the Rocas Verdes Formation and could suggest that GCN glaciers were still relatively extensive at this time (Kilian et al., 2007a).

Kilian et al. (2007b) used a parametric echo sounding system to detect sub-aquatic ridges interpreted as moraine systems in Euston and Gajardo channels. Although these mapped sub-aquatic moraines are undated, Kilian et al. (2007b) tentatively correlated them to glacial stages identified in Strait of Magellan Ice Lobe (namely Stages D and E; discussed in Section 5). The Euston Channel moraine limit is interpreted as 'Stage D' (~18 ka) based on the absence of further landforms between these moraines and the IRD layer in the SK1 core (dated to 17.46–18.28 ka BP*). This suggests rapid deglaciation with no standstills which would have been facilitated by the interpreted low glacier-surface slope. From palynological evidence from a sediment core (GC2) above Gajardo Fjord it has been inferred that the Gajardo Channel moraine (~12 km outside present-day ice extent) was likely occupied between 14.13 and 11.02 cal ka BP. A minimum age of 12.12 cal ka BP indicates ice-free conditions on Chandler Island (core CH1). Hence, the Gajardo Channel moraine is constrained to 14.13–12.12 cal ka BP, and Kilian et al. (2007b) interpret the readvance as coeval with the Late glacial 'Stage E' of Strait of Magellan Ice Lobe, during the Antarctic Cold Reversal (ACR; 14.7-13 ka; Pedro et al., 2016).

4. Seno Otway Ice Lobe

Seno Otway Ice Lobe flowed northeast from Santa Inés Icefield (SII), advancing over 200 km from the present-day icefield during the lLGM (Figs. 1 and 2). The terminal moraines of this ice lobe are a series of distinct arcuate ridges but the chronology is poorly constrained, with no direct dating of these maximum last glacial cycle limits (Darvill et al., 2017). However, the orientation and distribution of drumlins and lateral-terminal moraines north of Punta Arenas indicate that Seno Otway Ice Lobe joined Strait of Magellan Ice Lobe during its maximum extent (Benn and Clapperton, 2000a; Darvill et al., 2017; De Muro et al., 2018; Kilian et al., 2013; Lovell et al., 2012). Terrace systems along the shores of Seno Otway, Seno Skyring and Última Esperanza (north of Seno Skyring; see Fig. 1A) indicate that, during retreat from this maximum, a large 5700 km^2 interconnected proglacial lake formed in front of the retreating ice lobes (Kilian et al., 2013). A cosmogenic ^{10}Be depth profile through outwash associated with a drainage channel along a southeastern spillway constrains the timing for partial drainage of Laguna Blanca Lake from Seno Skyring to 22 ± 3 ka (Lira et al., 2022). This represents a minimum age for deglaciation from the lLGM of Seno Otway Ice Lobe as the drainage channel cuts through moraine system east of Seno Otway. A minimum age for complete lake drainage is constrained by a radiocarbon date of 14.2 ka BP* from a raised shoreline east of Seno Otway (Kilian et al., 2013), and a further radiocarbon date from basal organics in a peat core within an abandoned meltwater channel, which yielded an age of 14.58 ± 0.69 cal ka BP (Mercer, 1976). McCulloch et al. (2005b) observed the Volcan Reclus tephra overlying the basal clays and silts in the same abandoned meltwater channel, indicating complete lake drainage had occurred sometime before 15 cal ka BP. Kilian et al. (2013) retrieved a sediment core (OTW2) from the middle sector of Seno Otway, ~50 km southwest of the proglacial lake raised shoreline. Radiocarbon dating of basal organics suggested ice-free conditions by 14.78 ka BP*. However, basal organics from a lake core on Isla Santa Inés ~80 km further upstream (closer to the present icefield) yield a minimum age for deglaciation of 16.02 ± 0.18 cal ka BP (Fontana and Bennett, 2012), suggesting the Seno Otway dates are not close minimum-limiting ages for deglaciation. Likewise, cosmogenic ^{10}Be ages from erratic boulders and bedrock samples in Canal Jerónimo and northern Isla Santa Inés (green circles; Fig. 2) indicate deglaciation of these sites by ~16 ka (n = 5; McCulloch et al., 2024).

Table 1
Summary of the geomorphological and geochronometric evidence for and against the outer glacial limits (RC, SdSS, PA & Stage A) being deposited during the last glacial cycle and representing a more extensive southern Patagonia glaciation during MIS 3 or MIS 4.

Evidence For	Reference
• Cosmogenic ^{10}Be exposure ages of boulders on RC, SdSS, PA and Stage A moraine crests date to the last glacial cycle (Fig.7)	Kaplan et al., 2007; 2008; Evenson et al., 2009; Peltier et al., 2021
• Cosmogenic ^{10}Be ages of surface cobbles on the outwash associated with the RC and SdSS moraine limits date to 25.6 ± 2.8 ka and 24.7 ± 1.0 ka	Darvill et al., 2015b
• Modelled age-depth profiles of outwash sediments associated with the RC and SdSS moraine limits date to 45.6 ka (+139.9/−14.3) and 30.1 ka (+45.6/−23.1)	Darvill et al., 2015b
Evidence Against	**Reference**
• Moraine morphology, soil development and weathering rind thickness is distinctly different between the Stage B-D inner moraines and the outer moraines, suggesting a significant time difference between their deposition	Bentley and McCulloch, 2005; Bentley et al., 2005; Clapperton et al., 1995; McCulloch et al., 2005a; Rabassa et al., 2000; Sugden et al., 2005
• Marine shells incorporated into the basal till of the Stage B moraine limit are dated to MIS 3, suggesting a complete deglaciation of the Strait of Magellan during the MIS 3 marine high stand	Clapperton et al., 1995; McCulloch et al., 2005a
• Marine shells incorporated into the basal till of the Stage A moraine limit imply a complete deglaciation of the Strait of Magellan between the deposition of the PA glacier limit and the Stage A glacier limit, likely during the MIS 5 marine high stand	Clapperton et al., 1995; McCulloch et al., 2005a

5. Strait of Magellan and Bahía Inútil ice lobes

Strait of Magellan and Bahía Inútil ice lobes together comprise the most well-studied of the southernmost PIS outlets. Strait of Magellan Ice Lobe flowed north from the ice divides near Isla Clarence and Isla Capitán Aracena and western CDI towards the Primera and Segunda Angosturas. Bahía Inútil Ice Lobe flowed north from the northern CDI, through Canal Whiteside, branching off northeast at Cabo Boqueroń (Fig. 3; and see Fig. 1 for wider geographical context).

The first extensive mapping of the glacial geomorphology of Strait of Magellan and Bahía Inútil ice lobes was conducted by Caldenius (1932). The development of radiometric-dating techniques, alongside additional geomorphological mapping, facilitated the glacial chronology of the region to be progressively better constrained over the second half of the 20th century (Anderson and Archer, 1999; Benn and Clapperton, 2000a, 2000b; Clapperton et al., 1995; Jackofsky et al., 2000; McCulloch and Bentley, 1998; Meglioli, 1992; Porter, 1990; Porter et al., 1992; Prieto and Winslow, 1994; Uribe, 1982). Clapperton et al. (1995) proposed a chronological framework for the five innermost glacial limits of the two ice lobes, terming them Stages A-E, from oldest to youngest. This chronology was subsequently refined by McCulloch et al. (2005a) using tephrochronology, cosmogenic ^{10}Be dating, amino-acid racemisation (AAR) and radiocarbon dating. In this section, we also use the Stage A-E naming convention and attempt to summarise the addition of subsequent studies into this framework (e.g. Bentley et al., 2005; Blomdin

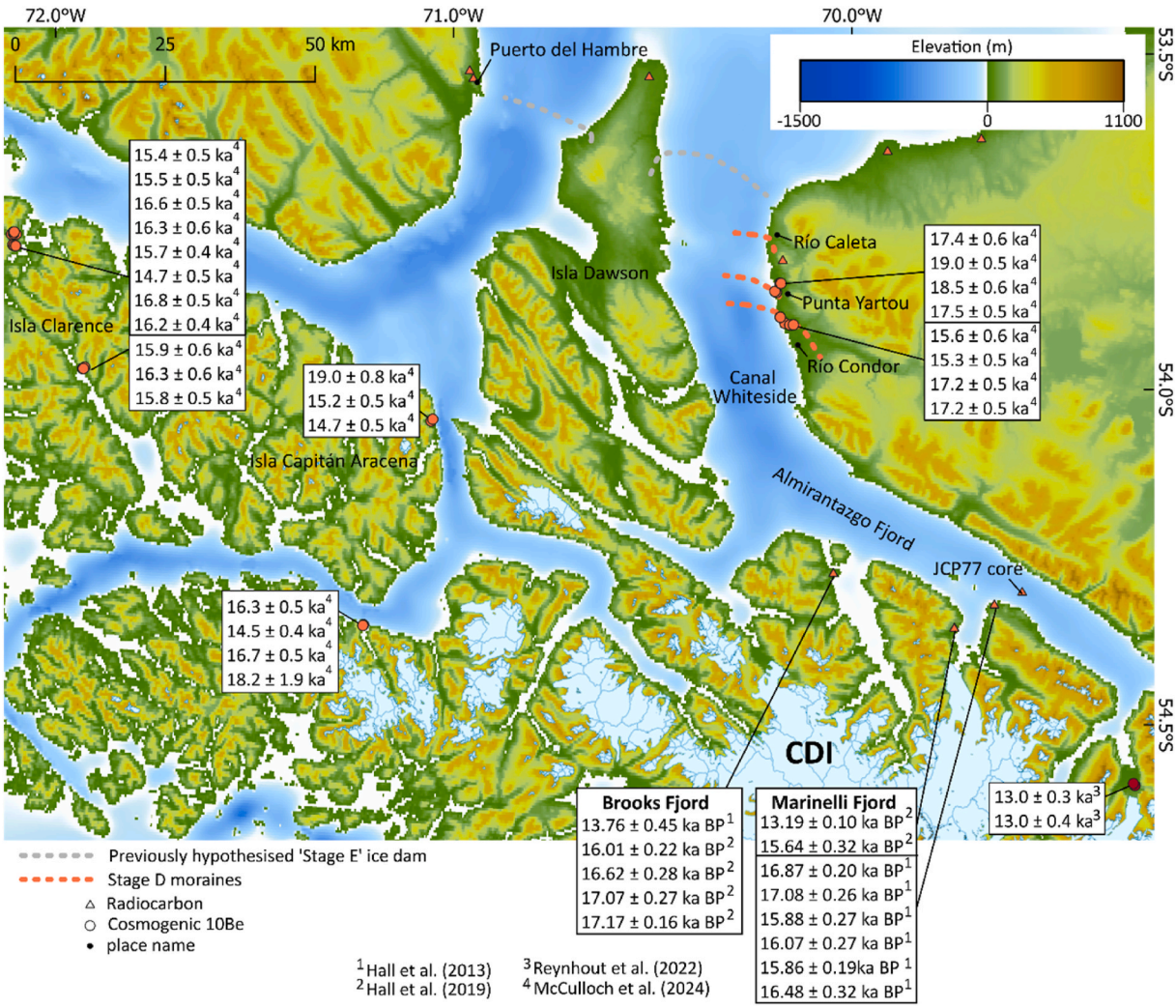

Fig. 4. The locations of previously mapped moraines and geochronometric dates relating to deglaciation, brief glacier standstills and readvances during the ACR in Canal Whiteside and the northern CDI, displayed on the ETOPO 2022 15 Arc-Second Global Relief Model.

et al., 2012; Boyd et al., 2008; Darvill et al., 2015a, 2015b; De Muro et al., 2018; Evenson et al., 2009; Fernández et al., 2017; Glasser and Jansson, 2008; Hall et al., 2013, 2019; Kaplan et al., 2007, 2008; Lovell et al., 2012; McCulloch et al., 2024; Moreno et al., 2023; Peltier et al., 2021; Reynhout et al., 2022; Sagredo et al., 2011; Soteres et al., 2020). In addition, we review the evidence that the outer glacial limits (Río Cullen, Sierras de San Sebastián and Primera Angostura, see Fig. 3), previously hypothesised to be deposited during MIS 12, 10 and 6 (Meglioli, 1992), were also deposited during the last glacial cycle. A summary of this evidence is presented in Table 1.

5.1. *Río Cullen and Sierras de San Sebastián moraine limits*

There has been debate in the literature concerning whether the Río Cullen (RC) and Sierras de San Sebastián (SdSS) moraine limits (Fig. 3) were deposited during the last glacial cycle or during an earlier glacial cycle. An age model hypothesised by Meglioli (1992) suggested that the RC moraines were deposited during MIS 12 (MIS 12–424–478 ka; Lisiecki and Raymo, 2005). This was based on the age bracketing of glacial till between basalt lava flows dated using $^{40}Ar/^{39}Ar$ dating to between 1.07 Ma and 0.45 Ma (Fig. 3). In the absence of further absolute dating constraints, Meglioli (1992) tentatively assigned the SdSS moraines to MIS 10 (MIS 10–374-337 ka; Lisiecki and Raymo, 2005) because the difference in moraine morphology and weathering-rind development suggested it represented a subsequent glaciation. Initially, this age model was widely accepted; detailed and consistent field observations by subsequent authors (e.g. Bentley et al., 2005; Clapperton et al., 1995; McCulloch and Bentley, 1998; McCulloch et al., 2005a; Rabassa et al., 2000) reported pronounced differences in weathering characteristics between the well-preserved, sharp-crested gLGM landforms (Stage B-D moraine limits) and the thick loess deposits and subdued topography of landforms outboard of these moraines. These observations were used to infer a significant age difference between the 'inner' (Stage B-D) and 'outer' (Stage A, PA, SdSS, RC) moraines, corroborating the assertion that the RC and SdSS moraines were deposited prior to the last glacial cycle. However, it is noted, that this relative dating based on differences in moraine morphology is not underpinned by well-constrained knowledge of rates of landform change in this region. In addition, Clapperton et al. (1995) and McCulloch et al. (2005a) observed shell fragments, some from identifiable species, within the tills associated with both the Stage A and Stage B moraine limits. AAR ages (corroborated by two infinite radiocarbon ages) constrain the age of the marine shells in the Stage A till to 130-90 ka (MIS 5). Ten radiocarbon ages (49.06–31.97 cal ka BP; one infinite age) and seven AAR ages (~35 ka) on the marine shells in the Stage B till all date to MIS 3 (Clapperton et al., 1995). These observations and chronological constraints indicate that the Strait of Magellan was ice-free and open to the Pacific Ocean during both MIS 5 and MIS 3, before the Stage A and B glacial readvances remobilised and incorporated the shells into their basal till. Since global sea level was at least 30 m lower

than present during MIS 3 (and between 116 and 134 m lower at the global LGM; Gowan et al., 2021; Lambeck et al., 2014), a marine incursion from the Atlantic Ocean would have been precluded by the area between the Segunda and Primera Angosturas. Therefore, a reduced glacial extent enabling marine incursion from the Pacific is the most plausible explanation for the origin of these shells. This leads to the inference that the Stage A moraine must have been deposited prior to the last marine high-stand that occurred during MIS 3, and the PA, SdSS and RC moraines must have been deposited prior to the penultimate marine high-stand during MIS 5. Therefore, the presence of dated marine shells in the basal till of the Stage B and Stage A moraines provide further evidence that the SdSS and RC moraines were deposited prior to the last glacial cycle.

However, recent advances in cosmogenic ^{10}Be dating have challenged this chronology. Dates from erratic boulders associated with RC and SdSS moraines in Bahía Inútil Ice Lobe suggested that the moraines may have been deposited during the last glacial cycle (Evenson et al., 2009; Kaplan et al., 2007). Eight out of twelve samples from Kaplan et al. (2007) yielded cosmogenic ^{10}Be ages <30 ka, with four anomalously old ages of 54.3 ka, 56.6 ka, 208.7 and 164.2 ka. All five of the samples from Evenson et al. (2009) yielded ages between 38 and 74 ka*. Both studies concluded that these anomalously 'young' ages were a result of intense episodic erosion during glacial periods, agreeing with the earlier studies that the RC and SdSS limits were deposited prior to the last glacial cycle. However, Darvill et al. (2015a) demonstrated, from making 5000 Schmidt Hammer measurements, no significant difference in hardness, and by inference, weathering characteristics between the 'young' and 'old' boulders, suggesting that they were all likely to have been deposited during the same glacial cycle. Since the existing cosmogenic ^{10}Be dates from boulders were generally 'too young' and scattered, Darvill et al. (2015b) applied cosmogenic ^{10}Be and ^{26}Al dating to glacial outwash cobbles associated with the moraines because these have been shown to more closely date older glacier limits where moraine degradation and boulder erosion cause scattered and 'too young' cosmogenic ^{10}Be ages (Hein et al., 2009). Following the methods of Hein et al. (2009), Darvill et al. (2015b) measured ^{10}Be and ^{26}Al concentrations of outwash surface cobbles and a ^{26}Al/^{10}Be depth-profile through the outwash sediments of both the RC and SdSS moraines (Fig. 3). The results yielded weighted mean exposure ages of 25.6 ± 2.8 ka (n = 3; one outlier removed) and 24.7 ± 1.0 ka (n = 4) for the outwash cobbles from the RC and SdSS moraines, respectively, and 45.6 ka ($^{+139.9}_{-14.3}$) and 30.1 ka ($^{+45.6}_{-23.1}$) for the corresponding modelled age-depth profiles. Since surface cobbles are considered to provide minimum-limiting ages, the study concluded that the absolute age of the RC and SdSS moraine limits linked them to deposition during MIS 3, indicating an earlier and more extensive maximum during the last glacial cycle. Further cosmogenic ^{10}Be dating of moraine boulders by Peltier et al. (2021) on the right lateral moraine of Strait of Magellan Ice Lobe, which yielded a weighted mean age of 65.3 ± 1.1 ka (n = 5; Fig. 4) for the outer limit, suggested moraine deposition during MIS 4 (MIS 4–71-57 ka; Lisiecki and Raymo, 2005).

5.2. Primera Angostura moraine limit

Another moraine previously accepted to have been deposited during a prior glacial cycle is the Primera Angostura (PA) moraine limit, ~50 km inboard of the RC and SdSS moraines (e.g., Meglioli, 1992; Rabassa et al., 2000). Based on its morphostratigraphic position and weathering development, it was suggested that the PA limit was likely deposited during MIS 6 (Coronato et al., 2004; Meglioli, 1992; Rabassa and Coronato, 2009). This corroborates with the presence of the MIS 5 marine shells in the basal till of the Stage A moraine, implying that the PA moraine limit was deposited prior to MIS 5 (Clapperton et al., 1995).

However, four boulders sampled from the PA terminal moraine on PA peninsula (Fig. 3) yielded a weighted mean age of 24.4 ± 0.9 ka (n = 3; outlier of 35.2 ± 3.9 ka removed; Kaplan et al., 2007). Subsequently, Soteres et al. (2020) mapped in detail the right lateral moraine complex of Strait of Magellan Ice Lobe south of Peninsula Juan Mazía. Their mapping demarcated the complex pattern of multiple lateral moraine limits and identified a ridge corresponding with the moraine limit that wraps around PA Peninsula. Peltier et al. (2021) sampled four boulders from this lateral moraine ridge, which yielded a weighted mean age of 23.9 ± 1.9 ka (n = 4). Within error, this is consistent with earlier cosmogenic ^{10}Be dating of the terminal moraine by Kaplan et al. (2007).

As discussed for the RC and SdSS moraines, these apparently 'young' cosmogenic ^{10}Be dates for the PA moraines are at odds with the distinct difference in morphology between the inner (Stages B-D) moraines and these outer (Stage A, PA, SdSS and RC) moraines. Addressing this issue, Peltier et al. (2021) suggested that the higher degree of weathering observed in the outer limits could be explained by the proximity of these landforms to the glacier margin for ~7000 years whilst the ice lobe was terminating at its gLGM position. As with the RC and SdSS moraine limits, whether the PA moraine was deposited prior to or during the last glacial cycle is an ongoing debate in the literature (Table 1).

5.3. Stage A moraine limit (Strait of Magellan Ice Lobe)

The Stage A moraine limit comprises a subdued moraine complex observed northeast of Seno Otway and north of Peninsula Juan Mazía (Clapperton et al., 1995; McCulloch et al., 2005a; Prieto and Winslow, 1994; Rabassa et al., 2000; Raedeke, 1978, Fig. 3). Geomorphological mapping by Bentley et al. (2005) identified a clear morphological distinction between this moraine limit and its inboard landforms and sediments (i.e., the Stage B-D moraines), supporting the previously-accepted view that a significant time had passed between the Stage A event and Stages B-D (Clapperton et al., 1995; Meglioli, 1992).

A radiocarbon age from buried wood in the upper layer of the Stage A diamict suggests a maximum limiting age of glacier advance of 27.32 ± 0.86 cal ka BP, although the geological link between the moraine limit and sampled wood is unclear (Prieto and Winslow, 1994). However, the more recent application of cosmogenic ^{10}Be to moraine boulders corroborates the suggestion that the Stage A moraine limit was deposited more recently that initially thought. Five cosmogenic ^{10}Be ages from the right lateral moraine of Strait of Magellan Ice Lobe have a weighted mean of 23.5 ± 0.6 ka (Peltier et al., 2021). These upper lateral moraine dates can be tentatively traced to the Stage A moraine using the geomorphological mapping from Soteres et al. (2020) and Darvill et al. (2014). As described in the previous sections, these cosmogenic ^{10}Be ages suggest Stage A moraine deposition subsequent to the MIS 3 marine high-stand, which contradicts the evidence for two marine incursions recorded in the basal till of both the Stage B and Stage A basal tills.

5.4. Stages B-D moraine limits

The Stage B, C and D moraines are well-studied and prominent moraine crests widely agreed to have been deposited at Strait of Magellan and Bahía Inútil ice-lobe fronts during MIS 2 (Clapperton et al., 1995, Fig. 3). The Stage B and C moraines that terminate on Peninsula Juan Mazía can be traced across to the hillsides just above Punta Arenas to the west and curving around into Bahia Inútil to the southeast (Bentley et al., 2005; Clapperton et al., 1995; De Muro et al., 2018; McCulloch et al., 2005a). The prominent Stage B moraine is underlain by two earlier tills interbedded with stratified sediments, suggesting that successive glacier advances terminated close to the Stage B limit (Clapperton et al., 1995). On Peninsula Juan Mazía meltwater channels associated with Stage C cut through the Stage B moraine limits, showing that they are two distinct glacial events (Clapperton et al., 1995). Evidence of glaciotectonised Stage C moraines on the western shore of the Strait of Magellan suggests that Stage C represents a glacier readvance, rather than a standstill during retreat from the Stage B moraine (Benn and Clapperton, 2000a, 2000b). The Stage D moraine limit terminates at Punta Paulo and was traced across the submerged

Table 2
Weighted means of recalculated cosmogenic ^{10}Be ages pertaining to the Stage B-D moraine limits reported in McCulloch et al. (2005a), Kaplan et al. (2007, 2008) and Peltier et al. (2021).

Weighted Mean			Reference
Stage B	Stage C	Stage D	
26.1 ± 1.0 ka (n = 3)	21.6 ± 1.3 ka (n = 4)	18.5 ± 0.3 (n = 3)	McCulloch et al. (2005a)
N/A	20.0 ± 1.8 ka (n = 5)	N/A	Kaplan et al. (2007)
22.8 ± 3.6 ka (n = 5)	17.6 ± 3.0 (n = 1)	17.4 ± 1.8 (n = 6)	Kaplan et al. (2008)
18.8 ± 0.6 ka (n = 3)	17.9 ± 0.4 (n = 3)	17.5 ± 0.6 (n = 2)	Peltier et al. (2021)

bed of the Strait of Magellan using marine geophysics (Bartole et al., 2008; Fernández et al., 2017). The Stage D limit is a low and narrow ridge crest, only a few metres in elevation above the surrounding topography (Benn and Clapperton, 2000; Bentley et al., 2005; Darvill et al., 2014; Lovell et al., 2012).

Deposition of the Stage B-D moraine limits has been extensively dated using radiocarbon, AAR, tephrochronology, OSL and cosmogenic ^{10}Be dating (Blomdin et al., 2012; Clapperton et al., 1995; Evenson et al., 2009; Kaplan et al., 2007, 2008; McCulloch et al., 2005a; Peltier et al., 2021; Porter, 1990; Porter et al., 1992; Prieto and Winslow, 1994). Although precise ages for moraine formation are a little inconsistent between studies, there is convergence that the Stage B-D moraines were deposited during MIS 2. The weighted means of cosmogenic ^{10}Be ages for Stages B-D are summarised in Table 2. Blomdin et al. (2012) used K-feldspar Infrared-Stimulated Luminescence to date the deglaciation of a sample between the Stage C and D limits. Two minimum age models suggested, although with large associated uncertainties, ages of 22 ± 6 ka and 22 ± 5 ka (Blomdin et al., 2012). Radiocarbon ages for the shells in the basal till of the Stage B moraine limit provide a maximum age of 49.06–31.97 cal ka BP (n = 10; Clapperton et al., 1995; McCulloch et al., 2005a).

5.5. Retreat from Stage D moraine limit

In response to the onset of warming at ~18-17 ka (Peltier et al., 2021), Strait of Magellan and Bahía Inútil ice lobes began to retreat from the Stage D moraine limit. An extensive dataset (n = 32) of minimum-limiting 'ice-free' radiocarbon ages from peat cores around the shores of the Strait of Magellan and Bahia Inútil (Clapperton et al., 1995; McCulloch et al., 2005a, 2024; McCulloch and Bentley, 1998; Moreno et al., 2023; Porter et al., 1984; supplementary data) indicates that the ice sheet responded rapidly to warmer conditions and retreat was underway before 17 ka.

During deglaciation from the Stage D limit, a proglacial lake formed in the overdeepened basin, dammed by the retreating glacier front. Raised shorelines, at 30–60 m a.s.l. around the Strait of Magellan, mark the extent of this Stage D proglacial lake, which drained eastward to the Atlantic. Eleven radiocarbon dates on basal peat above these glaciolacustrine sediments show that the ice lobe had retreated from the central Strait of Magellan before 16.16–15.05 cal ka BP, allowing the lake to drain to the Pacific (McCulloch et al., 2005a, 2024). The presence of the robustly dated Volcan Reclus tephra (15.0 ka; McCulloch et al., 2005b; Sagredo et al., 2011) sandwiched between these peat layers also corroborates that the Stage D proglacial lake had drained before 15 ka.

Initial deglaciation appears to have been punctuated by a series of brief standstills or small readvances, which are evidenced by smaller and fragmented recessional moraines within the Stage D limit in a region of shallow depths and low bathymetric gradient (Fernández et al., 2017, Fig. 3). These moraines have been observed both onshore (Bentley et al., 2005; McCulloch et al., 2024) and offshore (marine geophysical survey; Fernández et al., 2017). As the ice lobes retreated southwards, encountering deeper water and higher bathymetric gradients, the rate of deglaciation accelerated and recessional moraines are no longer observed (Fernández et al., 2017).

However, there is evidence for a final stabilisation of Bahía Inútil Ice Lobe near Punta Yartou (Fig. 4). Geomorphological mapping by McCulloch et al. (2024) and Glasser and Jansson (2008) identified at least four additional Stage D moraine ridges between Río Caleta and Río Condor. Sixteen boulders from these moraines yielded a wide range of cosmogenic ^{10}Be ages, likely as a result of nuclide inheritance, but, after removing outliers, the remaining data suggest moraine occupation at ~18 ka (McCulloch et al., 2024). Geophysical data also show a 90 m thick deposit of coarse ice-proximal sediments at a shallowing before the deeper trough of southern Canal Whiteside, supporting a period of ice stabilisation at the topographic constriction between Isla Dawson and Punta Yartou (Fernández et al., 2017). These likely represent the last depositional glacial landforms before retreat of the ice sheet to the fjords surrounding CDI. Due to the increased water depth and lack of glacial deposits in southern Canal Whiteside, it is likely that deglaciation occurred rapidly from this point.

Rapid ice-sheet collapse following the onset of deglaciation is supported by radiocarbon dating on the northern margin of CDI. Fourteen minimum-limiting ages for deglaciation obtained from cores indicate that glaciers had retreated close to the current icefield by ~17 cal ka BP (Fig. 4; Boyd et al., 2008; Hall et al., 2013, 2019). This is corroborated by 31 cosmogenic ^{10}Be dates from erratic boulders and bedrock samples across the western Fuegian archipelago, between CDI and SII (Fig. 4). The consistency of this extensive dataset suggests deglaciation to within these fjords had occurred by at least ~16 ka (n = 31; McCulloch et al., 2024). Within analytical uncertainties, these studies imply near-instantaneous retreat over a distance of ~150 km from the Stage D moraine limit to just outside the present-day ice extent. Given the very low surface gradients, and therefore driving stresses, of the palaeo-Strait of Magellan and Bahía Inútil ice lobes (estimated to be as low as ~7.5 m/km and <10 kPa respectively), and the fact they were calving into deep water, such a rapid response to climatic warming would be expected (Clapperton et al., 1995; Kaplan et al., 2008).

5.6. Late glacial readvances

There has been much debate in the literature in relation to Late glacial readvances of Strait of Magellan and Bahía Inútil ice lobes during the ACR. The presence of lacustrine sediments and associated raised shorelines observed on the western and eastern shores of the Strait of Magellan and Bahia Inútil and on northern Isla Dawson have previously been interpreted as evidence for a large proglacial lake that was dammed by a glacier readvance of ~80 km, preventing drainage of meltwater to the Pacific Ocean (McCulloch et al., 2005a, 2005b; Clapperton et al., 1995; McCulloch and Bentley, 1998; Bentley et al., 2005). The timing of this extensive glacier readvance, termed 'Stage E' (Figs. 3 and 4), was constrained by radiocarbon dating and tephrochronology immediately above and below the laminations of bluish-grey clays and silts observed in stratigraphic sections around the Strait of Magellan, suggesting the proglacial lake had existed between ~15 and 12.3 cal ka BP (McCulloch et al., 2005b, 2024).

However, there is significant evidence to contradict the occurrence of this previously hypothesised 'Stage E' ice dam. Firstly, an extensive glacier readvance into the deep troughs of the central Strait of Magellan and Canal Whiteside would have required a significant increase in accumulation to maintain a stable calving ice front in water depths exceeding 400 m (McCulloch and Bentley, 1998). Furthermore, Hall et al. (2013, 2019) observed no evidence of glacier readvance in the stratigraphy of peat cores sampled in the Marinelli and Brooks fjords on the northern margin of CDI, suggesting ice has remained close to the present ice margin since ~17 ka (Section 5.5; Fig. 4). The JPC77 marine core in Seno Almirantazgo also records ice-free conditions following deglaciation before ~15.63 cal ka BP (Boyd et al., 2008) and marine

Fig. 5. The locations of previously mapped and undated moraine limits for Lago Fagnano, Canal Beagle and Paso Mantellero ice lobes, displayed on the ETOPO 2022 15 Arc-Second Global Relief Model. Also displayed are the locations of sediment cores. The corresponding recalibrated radiocarbon ages from these cores can be found in the supplementary data The rectangular box north of Ushuaia shows the location of ACR cirque glaciers dated by Menounos et al. (2013).

geophysical surveys by Fernández et al. (2017) found no evidence of submerged moraines that could constitute the continuation of the proposed 'Stage E' moraine across Canal Whiteside. In addition, Reynhout et al. (2022) used cosmogenic ^{10}Be dating to show that glaciers readvanced only a few kilometres from the current ice extent in the northern CDI during the ACR. Two moraine boulders, sampled only ~3 km from the current glacier extent, were dated and both yielded cosmogenic ^{10}Be ages of 13.0 ka (Reynhout et al., 2022). Further investigating the possibility of this ice-dammed lake hypothesis, McCulloch et al. (2024; Fig. 4) collected 31 cosmogenic ^{10}Be samples from erratic boulders and bedrock across the western Fuegian Archipelago to determine possible positions of this 'Stage E' ice dam. They found that all samples had been exposed in a stable position for at least ~16 kyr, demonstrating that an ice dam substantial enough to dam meltwater drainage to the Pacific could not have existed during the ACR.

An alternative explanation for the observed raised-lake deposits, which is compatible with a reduced glacier extent since ~17 ka, is proposed by McCulloch et al. (2024). They suggest that the early and

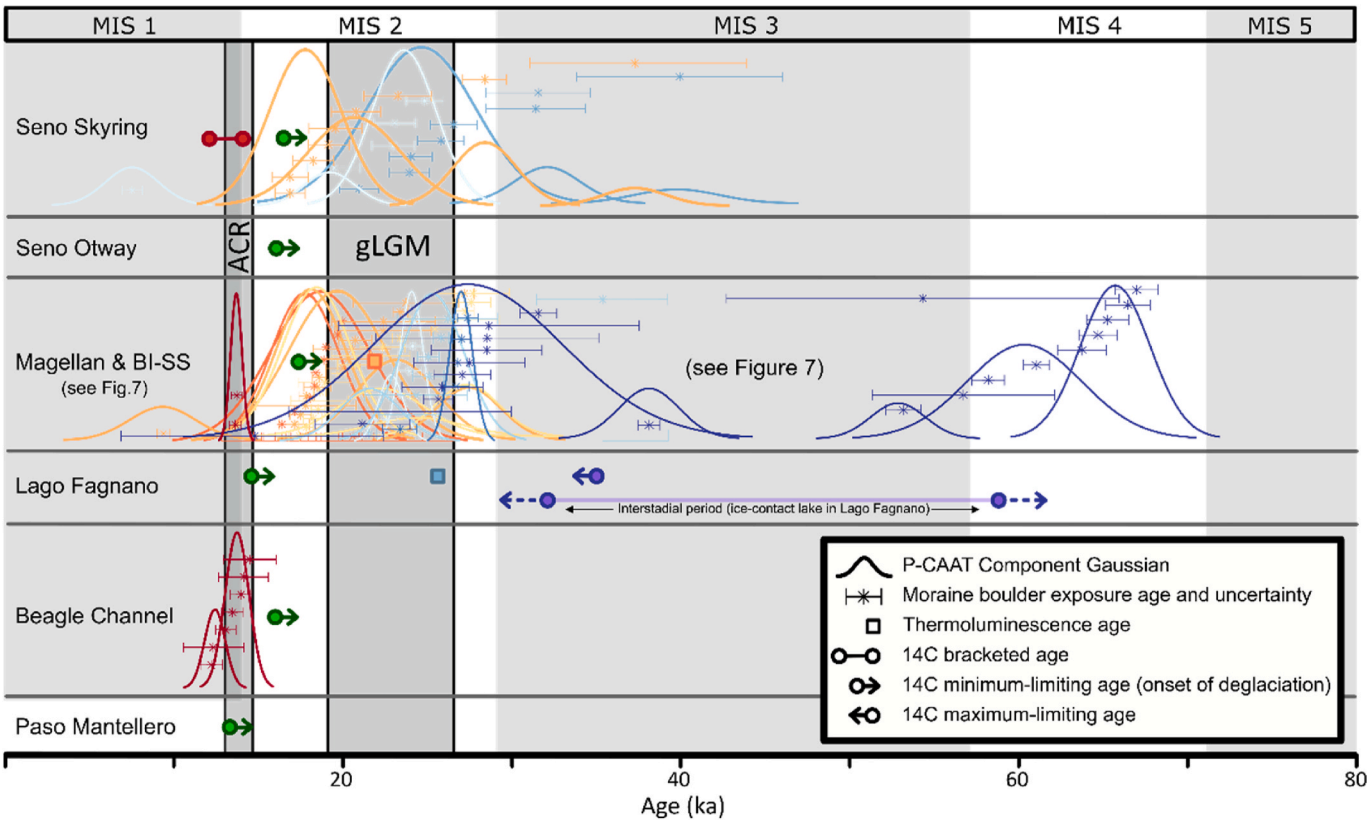

Fig. 6. Published dating constraints for the major outlets of the southernmost PIS during the last glacial cycle, displayed from north to south. Marine Isotope Stages are displayed in light grey (Lisiecki and Raymo, 2005). The ACR (Pedro et al., 2016) and gLGM (Clark et al., 2009) are displayed in dark grey. Individual cosmogenic ^{10}Be moraine boulder ages and uncertainties are shown, alongside the P-CAAT component Gaussians that describe their distribution. Colours correspond to the respective moraine limits in Figss. 2 and 3. All data are recalculated and can be found in the supplementary data alongside the choice of bandwidth estimator used to produce the P-CAAT Gaussians. Cosmogenic ^{10}Be ages from Strait of Magellan and Bahía Inútil ice lobes are shown in more detail in Fig. 7.

rapid collapse of the PIS in southernmost Patagonia resulted in rapid isostatic uplift of the shallow southern continental margins of the Fuegian Archipelago. By generating relative sea-level curves using a Glacial Isostatic Adjustment (GIA) model, they demonstrate that isostatic uplift between ~17 and 15 ka could have led to the formation of a land barrier on the continental shelf, damming the lake, which they name 'Lago Kawésqar'. McCulloch et al. (2024) also propose that the drainage of the raised lake at ~12 ka could be explained by neotectonic downfaulting of the southern land barrier along the Magellan-Fagnano Fault System (MFFS), a mechanism which had already been observed locally at Puerto del Hambre (Bentley and McCulloch, 2005). This vertical seismic displacement could explain the absence of palaeoshorelines and lacustrine sediments south of the MFFS, as they would be submerged below sea level as a result of ~30–50 m of downfaulting.

6. Lago Fagnano Ice Lobe

Lago Fagnano Ice Lobe flowed eastwards from CDI, reaching a total length of ~132 km during the last glacial cycle (Coronato and Rabassa, 2011; Waldmann et al., 2010, Fig. 5). At its maximum extent, ice covered an area of ~4000 km^2, with an eastward slope of 8° and a total ice volume of ~54 × 10^5 m^3, reaching a longitude of 66° 45' W (Coronato et al., 2009). Extensive geomorphological mapping of the region by Coronato et al. (2009) showed that an alpine-style glacial landscape fed by more than 50 tributary glaciers developed in the western part of Lago Fagnano. This transitioned to a lowland glacial landscape, forming a piedmont-type glacier in the eastern part of the lake basin.

The lack of datable material in the compact gravelly till that marks the maximum last glacial cycle extent of Lago Fagnano Ice Lobe makes chronological constraint challenging (Coronato et al., 2002, 2005). At its maximum extent, the main body of Lago Fagnano Ice Lobe branched into three outlets in the Fuego, Ewan and San Pablo valleys to the north, northeast and east of Lago Fagnano respectively (Coronato et al., 2009). This is evidenced by the mapping of 'ground moraine' and lateral till deposits that represent the eroded remnants of LGM moraines within these valleys (Coronato et al., 2008, 2009). These are the Buenos Aires, Miramonte, Penny and Yehuin moraines in the Fuego valley and the Indiana, Hantuk and Chepelmut moraines in the Ewan valley (Fig. 5). A fourth drainage route towards Sloggett Bay in the southeast was proposed by Bonarelli (1917) and Caldenius (1932) but later rejected by Coronato et al. (2009) as a local ice lobe draining from the Lucio López Range slopes. Divergence of Lago Fagnano Ice Lobe is further supported by seismic stratigraphic evidence of a sequence of five interpreted lateral or medial moraines, now submerged below the lake (Waldmann et al., 2010).

There are very few studies that date the past ice limits of Lago Fagnano Ice Lobe. A thermoluminescence age of 25.7 ka was obtained from the latero-frontal terminal moraine of Fuego Ice Lobe to the north of Lago Fagnano (Coronato et al., 2008, their table 51.2), suggesting maximum glacial conditions were obtained during the gLGM/MIS 2. The only other geochronological constraints are from stratigraphic profiles of glaciolacustrine deposits along the southeast shore of Lago Fagnano (Bujalesky et al., 1997; Coronato et al., 2009; Sanci et al., 2021; labelled 'stratigraphic profiles' in Fig. 5 and in order E-W). These sediments are interpreted by all authors to represent an ice-contact lake, likely dammed by Lago Fagnano Ice Lobe. The glaciolacustrine sequences are sandwiched between two glacial diamicts, suggesting that the ice-contact lake was preceded and succeeded by a glacier advance beyond the eastern shore of Lago Fagnano. Radiocarbon dating of peat

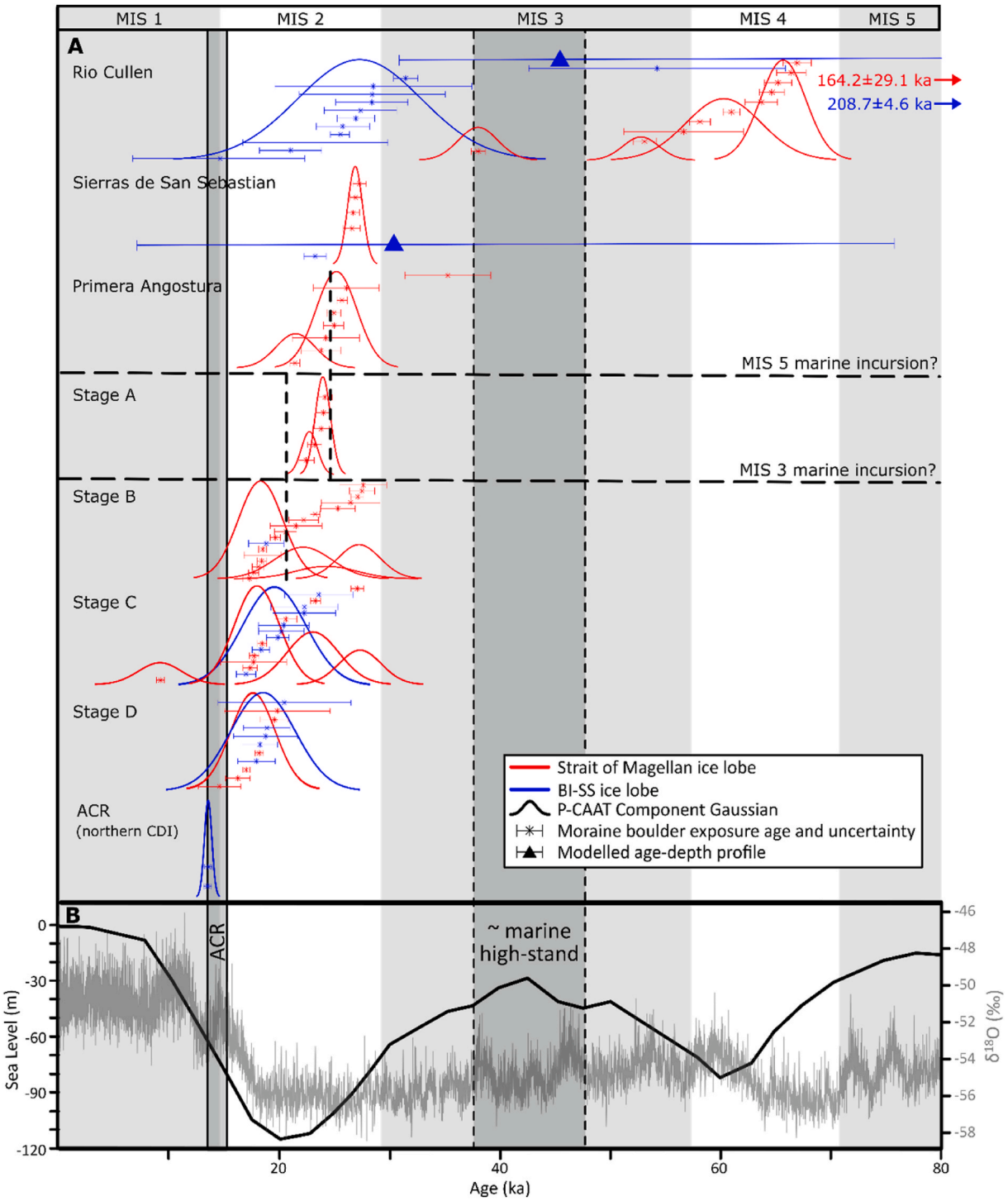

Fig. 7. (A) Published cosmogenic ^{10}Be moraine boulder ages for Strait of Magellan and Bahía Inútil ice lobes during the last glacial cycle from outermost (oldest) to innermost (youngest). Annotations of marine isotope stages, ACR and gLCM (grey boxes), individual boulder ages and uncertainties, and P-CAAT statistics are symbolised as for Fig. 6. The presence of marine shells in the basal till of the Stage B and A moraines imply marine incursions (and, therefore, an ice-free Strait of Magellan) represented by horizontal dashed lines. However, the 'young' cosmogenic ^{10}Be ages of the outer (Stage A, PA, SdSS and RC) moraines would imply that these marine incursions occurred during the MIS 2 marine low stand (corresponding vertical dashed line), an unlikely scenario involving implausibly dynamic glacier fluctuations over 100s of kms during a period of relative climate stability. If the presence of these marine shells has been interpreted correctly, the cosmogenic ^{10}Be ages from the Stage A moraine should plot to the right of the MIS 3 marine high stand (dashed dark grey box) and the ages for the PA, SdSS and RC moraines should plot to the right of the MIS 5 marine high stand (off the scale shown here). I.e., the published cosmogenic ^{10}Be ages and interpretation of marine shells in the basal till are incompatible and imply drastically different last glacial cycle chronologies. Note that the Stage D dataset does not include ages from recessional moraines. (B) Reconstructed global sea level (Gowan et al., 2021) and the δ^{18}O record from EPICA dome C (Lambert et al., 2012).

in the glaciolacustrine deposits elicited maximum limiting ages for the uppermost diamict (and minimum limiting ages for the lowermost diamict) of 35.44 ± 0.95 cal ka BP and 49.75 ± 5.24 cal ka BP and four infinite ages (Bujalesky et al., 1997; Coronato et al., 2009). Sanci et al. (2021) used an age-depth model constrained by five radiocarbon ages to suggest deposition of these glaciolacustrine deposits between 49 and 32 cal ka BP. The authors extrapolate this sedimentation rate to the full depth of the sedimentary sequence, as determined by geophysical surveys (Prezzi et al., 2019), to infer the presence of an ice-contact lake as early as 58.8 cal ka BP. This suggests, as proposed by Bujalesky et al. (1997) and supported by later authors, that the preceding glacier advance took place during MIS 4 (although possibly MIS 6) and the subsequent overriding diamict records a glacier advance during MIS 2. The ice-contact-lake deposits sandwiched between these two glacial diamicts indicate that, although Lago Fagnano Ice Lobe was less extensive during MIS 3, it likely remained in contact with Lago Fagnano throughout this interstadial period and did not retreat to Almirantazgo Fjord before the MIS 2 glacier advance. This is evidenced by the presence of dropstones, absence of sub-fossils and scarce organic matter within the stratigraphic profiles (Sanci et al., 2021). However, there is no indication of the position of the ice dam within Lago Fagnano, although the progressively more ice-distal facies and lake lowering described in the eight stratigraphic sections at the far eastern shore suggest that the ice margin continued to retreat progressively throughout MIS 3, allowing for partial drainage of the ice-dammed lake (Bujalesky et al., 1997).

Deglaciation of eastern Lago Fagnano following the MIS 2 glaciation occurred before 14.46 ± 0.39 cal ka BP, based on minimum radiocarbon ages from basal peat (Coronato et al., 2009). A substantial number of Late glacial moraines have been observed in, and along the shores of, Lago Fagnano. Coronato et al. (2009) mapped three recessional moraines (Tolhuin-Jeu Jepen moraine, Valdez moraine and Martinez moraines; Fig. 5) which were proposed to have been deposited during Late glacial recession from the glacier's maximum extent, but remain undated. Waldmann et al. (2010) used multi-channel seismic profiles along Lago Fagnano to identify and map a series of submerged frontal, central and lateral moraine crests preserved in the lake basin. These represent at least 20 readvances or standstills of Lago Fagnano Ice Lobe during retreat, suggesting a step-wise and prolonged deglaciation pattern. Submerged moraine C4, representing one of the final glacier readvances in the western Lago Fagnano basin, was estimated to have been deposited at ~11.2 ka. This was based on the onlap of a traceable seismic stratigraphic layer from a sediment core to the submerged C4 moraine. An age-depth model of the sediment core that was based on the H1 tephra (eruption of Mt Hudson at ~8 ka; Stern et al., 2016) and an estimated sedimentation rate, gave the approximate age of 11.2 ka, although the authors suggest that a lower sedimentation rate would equate to deposition during the ACR. Waldmann et al. (2010) suggested that final retreat of Lago Fagnano Ice Lobe from the Tierra Del Fuego lowlands towards the Cordillera Darwin occurred during the later stages of the Younger Dryas, following ACR weakening. This enabled the drainage of the lake westwards into the Pacific. Lake level was lowered as a consequence, subaerially exposing the glaciolacustrine sediments that are now found in cliff exposures along the lake shores (Waldmann et al., 2010). However, this estimated timing of glacial retreat from the western side of Lago Fagnano would appear to be a significant underestimate given the earlier timing of retreat into the fjords of the northern CDI before ~17 ka (Hall et al., 2013, 2019).

7. Canal Beagle Ice Lobe

Canal Beagle Ice Lobe flowed eastward from the southern and eastern CDI, exploiting a fault line that has been glacially overprinted throughout multiple glacial cycles (Fig.1; Fig.5). Although the timing of maximum extent of Canal Beagle Ice Lobe is based only on radiocarbon dating of basal peat, Rabassa et al. (2006) suggest maximum glacial conditions were attained at ~22-20 cal ka BP, during MIS 2. The ice lobe is thought to have reached ~1400 m ice thickness and terminated at the Punta Moat moraine complex, ~150 km from the modern glacier extent (Rabassa and Clapperton, 1990). This moraine complex is composed of several nested ridges that represent at least four standstills or small readvances, which suggests that the ice front remained close to its maximum glacial extent for some time (Rabassa et al., 1990). A well-developed drumlin flow-set has been mapped on Isla Gable and along the northern shore of Isla Navarino, and likely formed whilst the ice lobe terminated at Punta Moat (Rabassa et al., 2000).

The timing of deglaciation of Canal Beagle is much better constrained than its maximum extent. Seventeen peat cores, covering a transect of past ice-lobe extent, provide minimum-limiting radiocarbon ages for the retreat of Canal Beagle Ice Lobe (Fig. 5). The oldest minimum-limiting age constraint in the eastern Canal Beagle is a basal date of 17.84 ± 0.75 cal ka BP from Puerto Harberton (Heusser, 1989a). However, this core was likely sampled with a Hiller Borer which can cause potential issues with sample contamination (Jowsey, 1966). Two other cores from Puerto Harberton yielded basal ages of 16.10 ± 0.83 (Markgraf and Huber, 2010) and 15.99 ± 0.21 cal ka BP (Vanneste et al., 2015). At Lago Eugenia, Björck et al. (2021) reported a basal age of 15.04 ± 1.01 cal ka BP (although with inverted ages of 19.25 ± 0.38, 15.26 ± 1.04 and 15.52 ± 0.27 cal ka BP close above the basal age) and McCulloch et al. (2019) reported a basal age of 15.88 ± 0.17 cal ka BP from a coastal peat bog at Caleta Eugenia. Together, these radiocarbon ages from eastern Canal Beagle show that the ice lobe had already retreated at least 50 km from Punta Moat moraine before ~16 cal ka BP. A single radiocarbon age of 15.05 ± 0.43 cal ka BP was reported from Caleta Robalo in central Isla Navarino (Heusser, 1989b), but this again was likely sampled using a Hiller Borer so should be treated with caution. A minimum-limiting age of 17.12 ± 0.23 cal ka BP was reported at Punta Burslem (McCulloch et al., 2020), and two ages of 16.17 ± 0.27 and 15.97 ± 0.26 cal ka BP at Puerto Navarino (Björck et al., 2021). Three basal ages of 13.93 ± 0.13, 14.54 ± 0.40 and 13.92 ± 0.13 ka BP are also reported at Ushuaia 1, 2 and 3 respectively (Heusser, 1998), but these samples were also likely collected using a Hiller Borer. These minimum-limiting ages from central Canal Beagle suggest continued rapid deglaciation of a further 60 km at ~16 ka. Along the northwest arm of Canal Beagle, Hall et al. (2013) reported two ages of 14.71 ± 0.38 and 12.11 ± 0.33 cal ka BP from the southeast CDI and two ages of 10.45 ± 0.2 and 14.49 ± 0.47 cal ka BP from the southern CDI. These record final deglaciation of Canal Beagle Ice Lobe close to the current ice extent before ~14.5 ka. The persistence of periglacial tundra likely inhibited the growth of dateable organic matter at some of the eastern sites, thus its likely many of these dates are not close-limiting minimum ages (McCulloch et al., 2019) whereas the minimum ages from the western sites, located along the wetter end of the east-west precipitation gradient, probably reflect the timing of ice-free conditions more closely.

During retreat of the ice lobe from Punta Moat, the Beagle basin would have been isolated from the Atlantic and Pacific Oceans by shallow sills, which were flooded at ~11 ka (Bujalesky, 2011). A seismic profile along the Canal Beagle north of Isla Navarino shows that glacial diamict is overlain by sediments interpreted as glaciolacustrine deposits (Bujalesky, 2011). This suggests that a proglacial lake developed in front of the retreating Canal Beagle Ice Lobe. Final drainage of this lake would have occurred when the ice lobe retreated past the opening of Canal Murray, a shallow sill (~30 m deep) west of Isla Navarino. Radiocarbon dating from organic sediments overlying varved clays at three core sites along the northern shore of Isla Navarino suggests that the proglacial lake occupied the channel until just before ~16 ka (Björck et al., 2021).

Seismic reflection revealed evidence of a submerged frontal-moraine complex near Punta Segunda, Canal Beagle, approximately 18 km west of Ushuaia Airport, suggesting that ice-lobe recession was interrupted by periods of ice-front stabilisation (Bujalesky, 2011; Rabassa et al., 2000). Given the extensive dataset of 'ice-free' radiocarbon dates described above, which are broadly indistinguishable between the east and west extremes of Isla Navarino, it is unlikely that these glacial standstills were

occupied for any significant time. Therefore, these submerged recessional moraines likely represent brief standstills during periods of high sediment flux amidst an overall rapid retreat of Canal Beagle Ice Lobe (Rabassa et al., 2000).

Further evidence for rapid deglaciation is provided by two cosmogenic ^{10}Be ages from cirques north of Ushuaia (Menounos et al., 2013). The weighted mean age of 16.2 ± 0.8 ka suggests that ice was limited to high-altitude cirque glaciers by ~16 ka (Menounos et al., 2013). Inboard of these bedrock sample sites, Menounos et al. (2013) sampled boulders on moraine crests 0.85–2.5 km beyond the current glacier margins. The weighted mean age of 13.2 ± 0.7 ka (n = 7) suggests a small readvance of cirque glaciers coeval with ACR. This is supported by three minimum-limiting radiocarbon ages of 12.16 ± 0.28 cal ka BP, 12.01 ± 0.13 cal ka BP and 11.89 ± 0.69 cal ka BP from the same study area (Menounos et al., 2013). Following this minor Late glacial readvance, there was no evidence found for glacier advances outside of the Little Ice Age (LIA) limit during the Holocene (Menounos et al., 2013). This is supported by the transition from relatively cold and dry Late glacial conditions to the warmer Holocene climate between ~12.6 and 11.7 ka (McCulloch et al., 2020).

8. Paso Mantellero Ice Lobe

Paso Mantellero Ice Lobe is the southernmost major outlet of the former PIS studied to date, extending ~160 km south from the CDI to the west coast of Isla Hermite at 55.53°S (Hodgson et al., 2023, Fig. 5). Few studies have focussed on the glaciation of the southernmost islands of Cabo de Hornos National Park due to their remote location and challenging access. The only known geomorphological field campaign to be conducted on these islands (Hodgson et al., 2023) reported an absence of drift deposits and glacial landforms, concluding that the islands were not overridden by ice and glaciation was limited to the local cirques that were mapped remotely by Glasser and Jansson (2008). However, on the west coast of Isla Hermite, Hodgson et al. (2023) reported stratigraphic sections of glacial diamict overlain by peat. Clast orientation in the diamict indicated a N-S palaeo-flow direction, suggesting the glacial diamict resembled the eastern lateral margin of a topographically constrained N-S ice stream through the Paso Mantellero trough. This provided the first direct evidence for this southernmost PIS extent, which has previously been suggested by flow lines in the PATICE reconstruction (Davies et al., 2020) and by 16 out of 21 of the gLGM Paleoclimate Modelling Intercomparison Project (PMIP) model experiments by Yan et al. (2022). Radiocarbon dating of peat macrofossils immediately overlying the glacial diamict suggests that deglaciation occurred before 12.92 ka BP, but this is likely not a close minimum age due to the delayed onset of peat growth at high latitudes during the Late glacial (Hodgson et al., 2023).

9. Western ice-sheet limit

There is little direct evidence of the western limits of the PIS in southernmost Patagonia and few studies have investigated the glacial geomorphology within the fjords and islands of the western margin. Rodriguez et al. (2023) published a high-resolution geomorphological map covering a 1565 km^2 area to the west of GCN. They reported a landscape dominated by glacial erosional landforms likely formed under thick, warm-based ice. It is assumed that the ice-sheet margin extended to the continental-shelf break, as evidenced by seismic data collected along a latitudinal transect of the western margin (DaSilva et al., 1997). This would also be in keeping with other LGM ice sheets that are thought to have terminated at the shelf break (e.g. Bentley et al. (2014), Clark et al. (2022), Hughes et al. (2016) and Leger et al. (2024) for the Antarctic, British-Irish, Eurasian and Greenland ice sheets, respectively). In addition, it is plausible that the increasing elevation of the PIS and increasing accumulation on the western flanks (due to the strong prevailing SWWs) throughout the last glacial cycle would have resulted in a westward ice-divide migration late in the last glacial cycle (Mendelová et al., 2020; Sugden et al., 2002), which likely allowed the PIS to reach the Pacific continental shelf break. The timing of maximum ice-sheet extent on the western margin is constrained only by a few marine sediment cores (Fig. 1): ODP Site 1233 in northern Patagonia at 41°S (Kaiser et al., 2007), MR16-09 PC03 in central Patagonia at 46°S (Hagemann et al., 2024) and MD07-3128 in southern Patagonia at 53°S (Caniupán et al., 2011). Hagemann et al. (2024) and Kaiser et al. (2007) reconstructed the timing of PIS advances during the last glacial cycle by analysing terrigenous sediment within the cores, which is thought to be enhanced during extensive ice cover due to increased glacial erosion. Both studies reported a high glaciofluvial sediment flux at ~70-60 ka (MIS 4) and ~40-30 ka (late MIS 3) as well as during the gLGM (MIS 2). An abrupt decrease in sediment supply at ~18 ka suggests that the western margin of the PIS remained extensive, perhaps still terminating at the shelf break, until rapid deglaciation after 18 ka (Hagemann et al., 2024).

10. Discussion

We summarise schematically the published geochronometric constraints on the timing of glacier fluctuations during the last glacial cycle for the ice lobes described in this paper (Fig. 6). Our compilation represents a significant update to the 2020 PATICE database, incorporating 103 newly published cosmogenic ^{10}Be ages and 13 new radiocarbon ages from recent studies in southernmost Patagonia. In Fig. 7 we depict the moraine-boulder cosmogenic ^{10}Be ages from Strait of Magellan and Bahía Inútil ice lobes in more detail, highlighting the most prominent ongoing debate of the last glacial cycle in southernmost Patagonia - the contradictory evidence for the lLGM extent.

The glacial chronology of Seno Skyring Ice Lobe is relatively well constrained, with no available dating to indicate an earlier lLGM during MIS 3 or MIS 4 (Lira et al., 2022). Further investigation of the outer crests of the Laguna Blanca moraine complex (LBI and LBII; Fig. 2), perhaps by sampling an age-depth profile through the associated glacial outwash, or the outwash surface cobbles, could discern whether the entire moraine complex formed relatively synchronously, or if a similar glacial extent was attained earlier in the last glacial cycle.

The maximum extent of Seno Otway Ice Lobe, despite being indicated by prominent terminal moraine ridges, has not yet been dated, and the onset of its deglaciation is also poorly constrained (Darvill et al., 2017). However, the geomorphology would suggest that the outermost moraines in Seno Otway (Fig. 2) were formed contemporaneously with theouter moraines of Strait of Magellan Ice Lobe. Further geochronometric constraints from Seno Otway need to be acquired to constrain this chronology.

The glacial geomorphology and chronology of Strait of Magellan and Bahía Inútil ice lobes have been the focus of many published studies and the Stage A-E moraine naming convention has often been used to compare the timing of ice lobes across southernmost Patagonia (Fig.3; Fig.6). However, despite considerable efforts using a variety of dating techniques to constrain the timing of these ice-lobe fluctuations, the ages from each moraine are poorly clustered and a single agreeable chronology (particularly for the lLGM) remains unclear (Fig. 7). Furthermore, it is likely that catastrophic drainage of the Bahía Inútil proglacial lake during deglaciation formed complicated meltwater pathways that, together with large mass movements, obliterated much of the previous landform evidence at Cabo Boquerón. Therefore, it is possible that the correlation of 'synchronously' deposited moraines between the two ice lobes may be incorrectly interpreted, further compounding the interpretation of these poorly clustered cosmogenic ^{10}Be datasets.

Extensive geomorphological mapping, stratigraphic profiles and marine seismic profiles have been used to study the last glacial cycle of Lago Fagnano Ice Lobe (Fig. 5). However, few of these studies have provided geochronometric constraints. Although stratigraphic profiles provide evidence for two periods of glaciation beyond the eastern shore

of the lake, there is no age constraint on the earlier glacier advance and only a single thermoluminescence age for the subsequent period of glaciation during MIS 2. It is also unclear which glacier advance was most extensive. Additionally, further dating could help to discern whether Lago Fagnano Ice Lobe remained more extensive until the late Younger Dryas (Waldmann et al., 2010), considerably later than the widespread evidence of rapid and early (~16 ka) collapse found elsewhere in southernmost Patagonia.

The chronology of Canal Beagle Ice Lobe remains poorly constrained and its maximum last glacial cycle extent at Punta Moat is only hypothesised to be ~22-20 ka based on minimum radiocarbon ages from basal peat. Direct dating of the Punta Moat moraine would be a helpful addition to our understanding of southernmost PIS evolution.

Paso Mantellero Ice Lobe is thought to be the southernmost extent of the former PIS during the last glacial cycle, but its timing is constrained only by a Late glacial radiocarbon date which is assumed not to be close-limiting. The western ice-sheet limit is thought to have reached the continental shelf break and likely remained an extensive marine-based margin until ice-sheet collapse at ~18 ka. Collection and analysis of a marine core south of CDI could provide further insight into the timing of ice-sheet advances onto and retreat from the continental shelf at the southernmost ice-sheet margin. Given the disparity in dating constraints across southernmost Patagonia described here, the following summary largely draws upon the chronology of Strait of Magellan and Bahía Inútil ice lobes where the glacial chronology is more thoroughly constrained.

10.1. Early local LGM

The existing geochronology does not permit an unambiguous assessment of whether the ice lobes in southernmost Patagonia reached a lLGM prior to the gLGM. For Strait of Magellan and Bahía Inútil ice lobes, there are consistent datasets of cosmogenic ^{10}Be exposure ages (MIS 4; Peltier et al., 2021) and age-depth profiles through glacial outwash (MIS 3; Darvill et al., 2015b) that suggest a more extensive and earlier maximum extent during the last glacial cycle. These data corroborate with an extensive cosmogenic ^{10}Be dataset from Torres del Paine and Última Esperanza ice lobes immediately north of our study region (lower red box; Fig. 1) that record a lLGM extent during MIS 3 that was twice as extensive as the gLGM extent (Çiner et al., 2022; García et al., 2018; Girault et al., 2022; Sagredo et al., 2011). Likewise, the maximum last glacial cycle extents of Lago Argentino Ice Lobe (upper red box; Fig. 1) culminated at 44.5 ± 8.0 ka and at 36.6 ± 1.0 ka (Romero et al., 2024).

However, earlier studies have proposed that the Strait of Magellan was ice-free during MIS 3 and MIS 5, prior to the Stage B and Stage A glacier readvances respectively (Clapperton et al., 1995; McCulloch et al., 2005a). This is because a marine incursion into the strait is thought to be the most plausible explanation for the presence of marine shells in their basal tills. The distinct change in moraine morphology and weathering characteristics of the outer (RC, SdSS, PA and Stage A) and inner (Stages B-D) moraines, along with the accumulation of loess deposits overlying the outer moraines, are also cited as evidence of their deposition during different glacial cycles. These conflicting chronologies are demonstrated in Fig. 7, where the MIS 3 marine high-stand is expected to have occurred after the deposition of the Stage A moraine (and the MIS 5 marine high-stand after the deposition of the PA moraine). Instead, nearly all samples from the outer Stage A, PA, SdSS and RC moraines yield cosmogenic ^{10}Be ages that are younger than expected, post-dating the MIS 3 marine high-stand.

These two lines of evidence are contradictory and there is clearly a need for this existing chronology to be better understood. It is pertinent to consider alternative explanations for the 'young' cosmogenic ^{10}Be ages or the incorporation of these marine shells in the basal tills of the Stage B and Stage A moraines. It is also possible that there could be inherent problems with the dating constraint of the MIS 3 (MIS 5) marine shells, that are close to (beyond) the dating limit of radiocarbon. Radiocarbon dating of marine materials is associated with an additional source of uncertainty because ocean carbon is not in isotopic equilibrium with the atmosphere. Ocean water is typically slightly depleted in ^{14}C, resulting in older apparent ages compared to the radiocarbon dating of terrestrial materials. Although this marine reservoir effect (MRE) is accounted for in our methods by recalibrating all ages with the Marine20 calibration curve (Section 2.2), it uses a globally averaged MRE which may not be appropriate for latitudes south of 40°S (Davies et al., 2022; Heaton et al., 2020). Clapperton et al. (1995) also recognised that there were significant assumptions that were made in their AAR dating methodology for these marine shells. Firstly, the D/L ratios were not locally calibrated, thereby causing uncertainties in the absolute ages of at least ±40–50% (McCoy, 1987). Secondly, the rate of racemisation is highly temperature dependent and the thermal history of the site is poorly constrained. An average post-depositional temperature of 4 °C for all sites is assumed, but even a ±1.5 °C deviation from this assumed post-depositional temperature could result in a 25–30% error in the estimated AAR age (McCoy, 1987). Finally, racemisation rate can vary considerably between mollusc species and Clapperton et al. (1995) were able to identify only a few of the dated shell fragments, instead using the modern racemisation rate of the mollusc genus *Mya*, a common mollusc found in similar environments at high northern hemisphere latitudes (Miller, 1985). Nevertheless, regardless of the uncertainty in the ages of these marine shells, merely their presence in the basal till of the Stage A and B moraines is diagnostic of a marine environment prior to the deposition of both moraines. Considering global sea-level reconstructions (e.g. Gowan et al., 2021; Lambeck et al., 2014), this implies a considerable time interval between these glacial stages, or requires an alternative explanation for the incorporation of the shells in these tills (Fig. 7). In order for the Strait of Magellan to have been ice-free and open to the Pacific Ocean between the ~25, ~23.5 and ~18.5 ka cosmogenic ^{10}Be ages of the PA, Stage A and Stage B moraines (Fig. 7), would imply implausibly large ice-sheet fluctuations of >200 km in a few thousand years. Another knowledge gap that could shed light on this lLGM vs. gLGM contradiction is a better understanding of the rate of landform change in the region to enable quantification of the implied time gap between the deposition of the inner and outer moraines. In addition to better understanding the existing chronology, GIA modelling could be used to investigate the timing and extent of past ice loading in the region compared to the height and age of raised shorelines on the Atlantic coast.

Stratigraphic sections in eastern Lago Fagnano also suggest a glacier advance sometime before MIS 3, but it is not clear where is the corresponding moraine limit, only that it extended beyond the eastern shore of the lake (Bujalesky et al., 1997; Coronato et al., 2009; Sanci et al., 2021). In the absence of further chronological constraints, it is also possible that this diamict relates to a previous glacial cycle. There is currently no evidence of an earlier last glacial cycle maximum for Seno Skyring, Seno Otway, or Canal Beagle ice lobes, but this does not preclude the possibility that these ice lobes expanded beyond or to their gLGM positions during MIS 3 or 4 as they did in other parts of Patagonia (e.g. García et al., 2018; García et al., 2021; Romero et al., 2024). However, it is clear that further evidence is required to infer a ubiquitous PIS maximum that was earlier and more extensive than the gLGM in southernmost Patagonia.

10.2. Global LGM and deglaciation

During the gLGM, the seven ice lobes discussed in this paper advanced ~130–200 km from the present-day ice extent and it is assumed that the western margin terminated on the continental shelf break. In Seno Skyring, the outermost of these moraine limits was attained at ~26 ka, with some dating evidence of an advance at this time in Strait of Magellan, Bahía Inútil and Lago Fagnano ice lobes as well. This coincides with the broad pattern of increased glacial activity reported across the southern hemisphere mid-latitudes at this time (Darvill

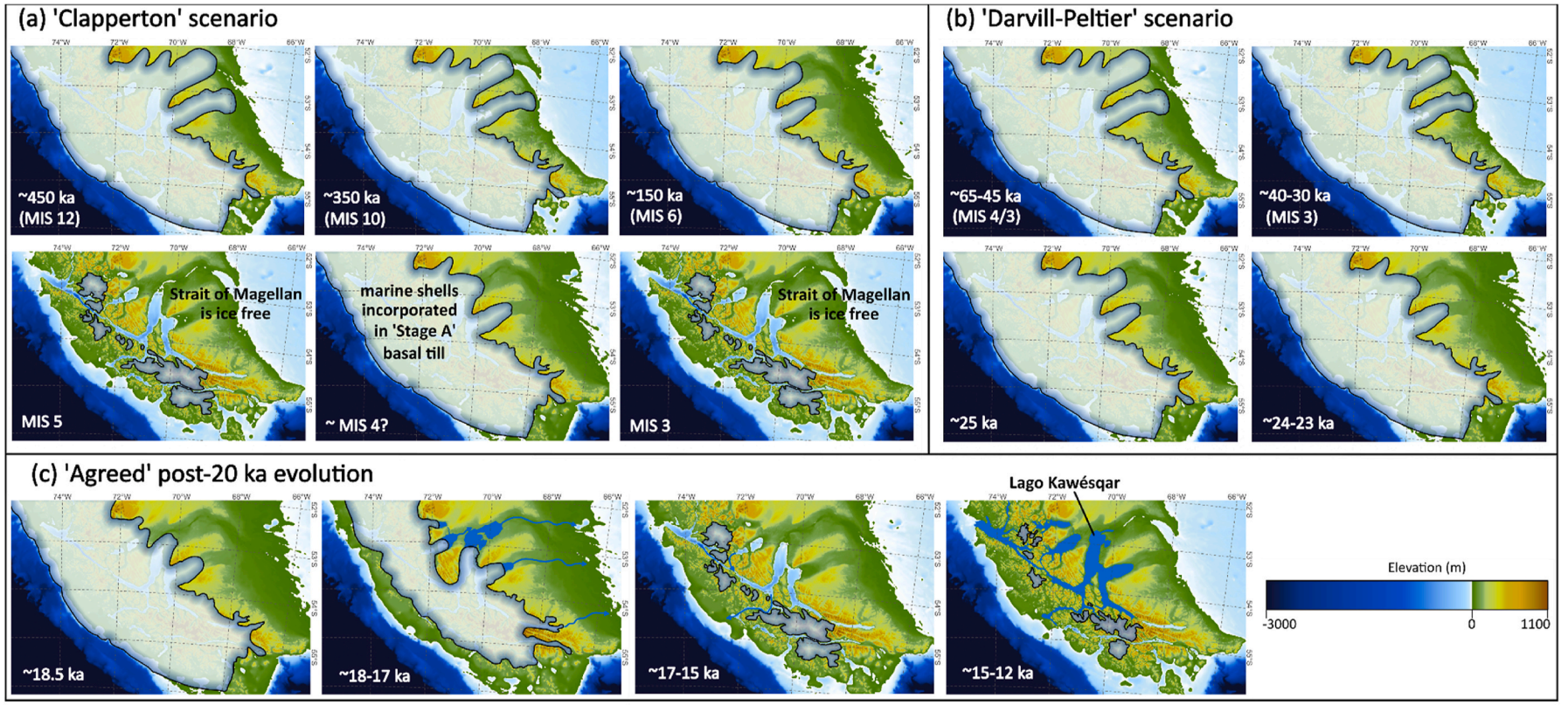

Fig. 8. Updated ice-sheet evolution for southernmost Patagonia. (a) the informally named 'Clapperton' scenario suggests that the outermost moraine limits were deposited prior to the last glacial cycle. This is based on the moraine morphology and weathering characteristics of the outer moraines and the marine shells incorporated into the basal tills of the Stage B and Stage A moraines (Bentley and McCulloch, 2005; Bentley et al., 2005; Clapperton et al., 1995; McCulloch et al., 2005a; Rabassa et al., 2000; Sugden et al., 2005). (b) the informally named 'Darvill-Peltier' scenario suggests that the outermost moraine limits were deposited within the last glacial cycle. This is based on Cosmogenic 10Be exposure ages from moraine crests and a modelled age-depth profile of outwash sediments associated with the outermost limits (Darvill et al., 2015b; Kaplan et al., 2007, 2008; Evenson et al., 2009; Peltier et al., 2021). (c) the post-20 ka ice-sheet evolution is the most well-constrained. At 18.5 ka the eastern ice lobes were still extensive and the western margin was likely a calving front on the continental shelf break. Rapid deglaciation of >150 km occurred before ~17 ka with no subsequent ice re-advances exceeding a few kilometres. The contradictory evidence for early and rapid deglaciation after Glacial Stage D and evidence for an ice dammed lake (Glacial Stage E) has been resolved. While the evidence for a high palaeolake 'Lago Kawésqar' between 15-12 ka is firm, it was dammed by an isostatically-uplifted land barrier that was breached by neotectonic downfaulting along the MFFS at ~12 ka (McCulloch et al., 2024). Relative sea level data are from Gowan et al. (2021) and displayed on the ETOPO 2022 15 Arc-Second Global Relief Mode.

et al., 2016). A series of moraine crests up to 30 km inboard of these limits date to the later stages of the gLGM and likely represent small readvances or glacier standstills. All of the ice lobes in southernmost Patagonia were still extensive until at least 18 ka, although there are limited chronological data to draw upon for Seno Otway Ice Lobe. The onset of deglaciation occurred after 18.1 ka in Seno Skyring, between 18 and 17 ka in Strait of Magellan-Bahía Inútil, before 17 ka in Canal Beagle and before 14.5 ka for Lago Fagnano. The deglaciation rate, inferred by the timing of retreat to the Fuegian fjords, appears to be rapid, reaching just outside the present-day icefields by ~16–17 ka on Isla Santa Inés, ~16 ka on Isla Clarence and Isla Capitán Aracena, by 17 ka in the northern CDI and by ~14.7 ka in the southern CDI. It is unlikely that retreat of Lago Fagnano Ice Lobe to the Fuegian fjords occurred later, during the Younger Dryas, as inferred by an estimated age for a submerged moraine (Waldmann et al., 2010). This would imply a contrasting response of Lago Fagnano Ice Lobe to the contemporaneous rapid and early retreat of the other southernmost PIS outlets. Rapid deglaciation is reported throughout many parts of the former PIS (e.g. Boex et al., 2013; García et al., 2019; Hein et al., 2010; Leger et al., 2021) and rapid collapse of the ice lobes in this region would be expected given the fact that they would have been calving into deep water and the low-angle glacier slopes and lower elevation of the Andes in southernmost Patagonia would have led to a high sensitivity to the onset of warmer conditions. Multiple submerged moraines have been detected in the glacial troughs of the former ice lobes, suggesting periods of glacial standstills during deglaciation. However, given the geochronometric evidence for rapid ice-sheet collapse to the Fuegian fjords, these recessional moraines could not have been occupied for a significant time period and more likely represent a high sediment supply.

10.3. Antarctic Cold Reversal

Glaciers surrounding GCN and CDI readvanced during the ACR, extending ~12 km in Gajardo Channel (52.8°S), ~3 km in the northern CDI (54.6°S), and <2.5 km in a small cirque glacier adjacent to Canal Beagle (54.7°S). This limited but coeval advance of glaciers during a period characterised by cooling in Antarctic ice cores is substantially smaller than the previously proposed ~80 km 'Stage E' readvance inferred from the presence of 'proglacial-lake' deposits and associated raised shorelines in the Strait of Magellan (McCulloch et al., 2005b). McCulloch et al. (2024) provides an alternative explanation for these observed raised-lake deposits, that is also compatible with the geochronological evidence, which suggests that any 'Stage E' glacier advances would not have been sufficient to dam a large lake in the Strait of Magellan and Bahía Inútil during the Late glacial. The moraines identified on Isla Dawson are recessional moraines from the Stage D limit, deposited during deglaciation before ~17 ka.

11. An updated ice-sheet reconstruction for southernmost Patagonia

Based on our updated compilation of geochronometric dates and in-depth review of existing and newly published literature since the PATICE reconstruction, we present in Fig. 8 an updated schematic of ice-sheet evolution in southernmost Patagonia. The informally named 'Clapperton' and 'Darvill-Peltier' scenarios show schematics of the two contradictory chronologies for the outermost moraine limits described in Sections 5.1-5.3 and summarised in Table 1.

CRediT authorship contribution statement

Carla Huynh: Conceptualization, Methodology, Writing, Visualization. **Andrew S. Hein:** Writing, Supervision. **Robert D. McCulloch:** Writing, Supervision. **Robert G. Bingham:** Conceptualization, Writing, Supervision.

Declaration of competing interest

The authors declare that they have no known competing financial interests or personal relationships that could have appeared to influence the work reported in this paper.

Data availability

Data is available in the supplementary zip file

Acknowledgements

This research was funded by an E4 DTP NERC Studentship (NE/S007407/1) awarded to CLH at the University of Edinburgh and the Chilean National Agency for Research and Development (FONDECYT 1200727 Agencia Nacional de Investigación y Desarrollo de Chile; ANID) awarded to RMcC. We thank Bethan Davies and an anonymous reviewer for their insightful comments which improved the final manuscript.

Appendix A. Supplementary data

Supplementary data to this article can be found online at https://doi.org/10.1016/j.quascirev.2024.108972.

References

Ammirati, J.-B., Flores, M.C., Ruiz, S., 2020. Seismicity along the Magallanes-Fagnano fault system. J. S. Am. Earth Sci. 103, 102799. https://doi.org/10.1016/j.jsames.2020.102799.

Anderson, D.M., Archer, R.B., 1999. Preliminary evidence of early deglaciation in southern Chile. Palaeogeogr. Palaeocl. 146 (1–4), 295–301. https://doi.org/10.1016/S0031-0182(98)00146-1.

Applegate, P.J., Urban, N.M., Laabs, B.J.C., Keller, K., Alley, R.B., 2010. Modeling the statistical distributions of cosmogenic exposure dates from moraines. Geosci. Model Dev. (GMD) 3 (1), 293–307. https://doi.org/10.5194/gmd-3-293-2010.

Applegate, P.J., Urban, N.M., Keller, K., Lowell, T.V., Laabs, B.J.C., Kelly, M.A., Alley, R.B., 2012. Improved moraine age interpretations through explicit matching of geomorphic process models to cosmogenic nuclide measurements from single landforms. Quaternary Res 77 (2), 293–304. https://doi.org/10.1016/j.yqres.2011.12.002.

Balco, G., Stone, J.O., Lifton, N.A., Dunai, T.J., 2008. A complete and easily accessible means of calculating surface exposure ages or erosion rates from 10Be and 26Al measurements. Quat. Geochronol. 3 (3), 174–195. https://doi.org/10.1016/j.quageo.2007.12.001.

Balco, G., 2011. Contributions and unrealized potential contributions of cosmogenic nuclide exposure dating to glacier chronology, 1990–2010. Quat. Sci. Rev. 30 (1–2), 3–27. https://doi.org/10.1016/j.quascirev.2010.11.003.

Balco, G., 2020. Glacier change and paleoclimate applications of cosmogenic-nuclide exposure dating. Ann. Rev. Earth Pl. Sci. 48, 21–48. https://doi.org/10.1146/annurev-earth-081619-052609.

Bartole, R., De Muro, S., Morelli, D., Tosoratti, F., 2008. Glacigenic features and tertiary stratigraphy of the magellan strait (southern Chile). Geol. Acta 6 (1), 85–100. https://doi.org/10.1344/105.000000243.

Benn, D.I., Clapperton, C.M., 2000a. Pleistocene glacitectonic landforms and sediments around central Magellan Strait, southernmost Chile: evidence for fast outlet glaciers with cold-based margins. Quat. Sci. Rev. 19 (6), 591–612. https://doi.org/10.1016/S0277-3791(99)00012-8.

Benn, D.I., Clapperton, C.M., 2000b. Glacial sediment–landform associations and paleoclimate during the last glaciation, Strait of Magellan, Chile. Quat. Res. 54 (1), 13–23. https://doi.org/10.1006/qres.2000.2140.

Bentley, M.J., McCulloch, R.D., 2005. Impact of neotectonics on the record of glacier and sea level fluctuations, Strait of Magellan, southern Chile. Geogr. Ann. A. 87 (2), 393–402. https://doi.org/10.1111/j.0435-3676.2005.00265.x.

Bentley, M.J., Sugden, D.E., Hulton, N.R.J., McCulloch, R.D., 2005. The landforms and pattern of deglaciation in the Strait of Magellan and Bahía Inútil, southernmost South America. Geogr. Ann. A. 87 (2), 313–333. https://doi.org/10.1111/j.0435-3676.2005.00261.x.

Bentley, M.J., Ó Cofaigh, C., Anderson, J.B., Conway, H., Davies, B., Graham, A.G.C., Hillenbrand, C.-D., Hodgson, D.A., Jamieson, S.S.R., Larter, R.D., Mackintosh, A., Smith, J.A., Verleyen, E., Ackert, R.P., Bart, P.J., Berg, S., Brunstein, D., Canals, M., Colhoun, E.A., Crosta, X., Dickens, W.A., Domack, E., Dowdeswell, J.A., Dunbar, R., Ehrmann, W., Evans, J., Favier, V., Fink, D., Fogwill, C.J., Glasser, N.F., Gohl, K., Golledge, N.R., Goodwin, I., Gore, D.B., Greenwood, S.L., Hall, B.L., Hall, K., Hedding, D.W., Hein, A.S., Hocking, E.P., Jakobsson, M., Johnson, J.S., Jomelli, V., Jones, R.S., Klages, J.P., Kristoffersen, Y., Kuhn, G., Leventer, A., Licht, K., Lilly, K., Lindow, J., Livingstone, S.J., Massé, G., McGlone, M.S., McKay, R.M., Melles, M., Miura, H., Mulvaney, R., Nel, W., Nitsche, F.O., O'Brien, P.E., Post, A.L., Roberts, S.

J., Saunders, K.M., Selkirk, P.M., Simms, A.R., Spiegel, C., Stolldorf, T.D., Sugden, D. E., van der Putten, N., van Ommen, T., Verfaillie, D., Vyverman, W., Wagner, B., White, D.A., Witus, A.E., Zwartz, D., 2014. A community-based geological reconstruction of antarctic ice sheet deglaciation since the last glacial maximum. Quaternary Science Reviews, Reconstruction of Antarctic Ice Sheet Deglaciation (RAISED) 100, 1–9. https://doi.org/10.1016/j.quascirev.2014.06.025.

Betka, P., Klepeis, K., Mosher, S., 2016. Fault kinematics of the Magallanes-Fagnano fault system, southern Chile; an example of diffuse strain and sinistral transtension along a continental transform margin. J. Struct. Geol. 85, 130–153. https://doi.org/10.1016/j.jsg.2016.02.001.

Björck, S., Lambeck, K., Möller, P., Waldmann, N., Bennike, O., Jiang, H., Li, D., Sandgren, P., Nielsen, A.B., Porter, C.T., 2021. Relative sea level changes and glacio-isostatic modelling in the Beagle Channel, Tierra del Fuego, Chile: Glacial and tectonic implications. Quat. Sci. Rev. 251, 106657. https://doi.org/10.1016/j.quascirev.2020.106657.

Blomdin, R., Murray, A., Thomsen, K.J., Buylaert, J.-P., Sohbati, R., Jansson, K.N., Alexanderson, H., 2012. Timing of the deglaciation in southern Patagonia: testing the applicability of K-Feldspar IRSL. Quat. Geochronol. 10, 264–272. https://doi.org/10.1016/j.quageo.2012.02.019.

Bonarelli, G., 1917. Tierra del Fuego y sus turberas. Buenos Aires, Argentina: Anales del Ministerio de Agricultura de la Nación, 12, Sección Geología Mineralogía y Minería.

Boyd, B.L., Anderson, J.B., Wellner, J.S., Fernández, R.A., 2008. The sedimentary record of glacial retreat, Marinelli Fjord, Patagonia: regional correlations and climate ties. Mar. Geol. 255 (3–4), 165–178. https://doi.org/10.1016/j.margeo.2008.09.001.

Bujalesky, G.G., 2011. The flood of the Beagle Valley (11,000 YR B.P.), Tierra del Fuego. An. Inst. Patagon. 39 (1), 5–21. https://doi.org/10.4067/S0718-686X2011000100001.

Bujalesky, G.G., Heusser, C.J., Coronato, A.M., Roig, C.E., Rabassa, J.O., 1997. Pleistocene glaciolacustrine sedimentation at Lago Fagnano, Andes of Tierra del Fuego, southernmost south America. Quat. Sci. Rev. 16 (7), 767–778. https://doi.org/10.1016/S0277-3791(97)00018-8.

Caldenius, C.C., 1932. Las glaciaciones Cuaternarias en la Patagonia y Tierra del Fuego. Geogr. Ann. 14 (1–2), 1–164. https://doi.org/10.1080/20014422.1932.11880545.

Caniupán, M., Lamy, F., Lange, C.B., Kaiser, J., Arz, H., Kilian, R., Baeza Urrea, O., Aracena, C., Hebbeln, D., Kissel, C., Laj, C., Mollenhauer, G., Tiedemann, R., 2011. Millennial-scale sea surface temperature and Patagonian Ice Sheet changes off southernmost Chile (53°S) over the past ~60 kyr. Paleoceanography 26. https://doi.org/10.1029/2010PA002049.

Çiner, A., Sarıkaya, M.A., Yıldırım, C., Girault, I., Todisco, D., Martin, F., Borrero, L., Fabel, D., 2022. Terrestrial cosmogenic 10Be dating of the Última Esperanza ice lobe moraines (52°S, Patagonia) indicates the global Last Glacial Maximum (LGM) extent was half of the local LGM. Geomorphology 414, 108381. https://doi.org/10.1016/j.geomorph.2022.108381.

Clapperton, C.M., Sugden, D.E., Kaufman, D.S., McCulloch, R.D., 1995. The last glaciation in central Magellan Strait, southernmost Chile. Quat. Res. 44 (2), 133–148. https://doi.org/10.1006/qres.1995.1058.

Clark, P.U., Dyke, A.S., Shakun, J.D., Carlson, A.E., Clark, J., Wohlfarth, B., Mitrovica, J. X., Hostetler, S.W., McCabe, A.M., 2009. The last glacial maximum. Science 325 (5941), 710–714. https://doi.org/10.1126/science.1172873.

Clark, C.D., Ely, J.C., Hindmarsh, R.C.A., Bradley, S., Ignéczi, A., Fabel, D., Ó Cofaigh, C., Chiverrell, R.C., Scourse, J., Benetti, S., Bradwell, T., Evans, D.J.A., Roberts, D.H., Burke, M., Callard, S.L., Medialdea, A., Saher, M., Small, D., Smedley, R.K., Gasson, E., Gregoire, L., Gandy, N., Hughes, A.L.C., Ballantyne, C., Bateman, M.D., Bigg, G.R., Doole, J., Dove, D., Duller, G.A.T., Jenkins, G.T.H., Livingstone, S.L., McCarron, S., Moreton, S., Pollard, D., Praeg, D., Sejrup, H.P., Van Landeghem, K.J. J., Wilson, P., 2022. Growth and retreat of the last British–Irish Ice Sheet, 31 000 to 15 000 years ago: the BRITICE-CHRONO reconstruction. Boreas 51, 699–758. https://doi.org/10.1111/bor.12594.

Coronato, A., Martínez, O., Rabassa, J., 2004. Glaciations in Argentine Patagonia, southern south America. In: Ehlers, J., Gibbard, P.L. (Eds.), Developments in Quaternary Sciences, Quaternary Glaciations Extent and Chronology. Elsevier, Amsterdam, pp. 49–67.

Coronato, A., Rabassa, J., 2011. Pleistocene glaciations in southern Patagonia and Tierra del Fuego. In: Ehlers, J., Gibbard, P.L., Hughes, P.D. (Eds.), Developments in Quaternary Sciences, Quaternary Glaciations - Extent and Chronology. Elsevier, Amsterdam, pp. 715–727.

Coronato, A., Seppälä, M., Ponce, J.F., Rabassa, J., 2009. Glacial geomorphology of the Pleistocene Lake Fagnano ice lobe, Tierra del Fuego, southern South America. Geomorphology 112 (1–2), 67–81. https://doi.org/10.1016/j.geomorph.2009.05.005.

Coronato, A., Roig, C., Mir, X., 2002. Geoformas glaciarias de la región oriental del Lago Fagnano, Tierra del Fuego, Argentina. In: XV Argentine Geological Congress (Vol. 2, Pp. 457-462). Minutes, Buenos Aires.

Coronato, A., Seppälä, M., Rabassa, J., 2005. Last Glaciation landforms in Lake Fagnano ice lobe, Tierra del Fuego, southernmost Argentina. In: VI International Conference on Geomorphology. International Association of Geomorphologists, vol. 22. Sociedad Española de Geomorfología, Zaragoza, Spain. Abstracts.

Coronato, A.M.J., Coronato, F., Mazzoni, E., Vázquez, M., 2008. The physical geography of Patagonia and Tierra del Fuego. In: Rabassa, J. (Ed.), The Late Cenozoic of Patagonia and Tierra del Fuego, Developments in Quaternary Sciences, vol. 11. Elsevier, Amsterdam, pp. 3–56. https://doi.org/10.1016/S1571-0866(07)10003-8.

Darvill, C.M., Bentley, M.J., Stokes, C.R., 2015a. Geomorphology and weathering characteristics of erratic boulder trains on Tierra del Fuego, southernmost South America: Implications for dating of glacial deposits. Geomorphology 228, 382–397. https://doi.org/10.1016/j.geomorph.2014.09.017.

Darvill, C.M., Bentley, M.J., Stokes, C.R., Hein, A.S., Rodés, Á., 2015b. Extensive MIS 3 glaciation in southernmost Patagonia revealed by cosmogenic nuclide dating of outwash sediments. Earth Planet Sci. Lett. 429, 157–169. https://doi.org/10.1016/j.epsl.2015.07.030.

Darvill, C.M., Bentley, M.J., Stokes, C.R., Shulmeister, J., 2016. The timing and cause of glacial advances in the southern mid-latitudes during the last glacial cycle based on a synthesis of exposure ages from Patagonia and New Zealand. Quat. Sci. Rev. 149, 200–214. https://doi.org/10.1016/j.quascirev.2016.07.024.

Darvill, C.M., Stokes, C.R., Bentley, M.J., Evans, D.J.A., Lovell, H., 2017. Dynamics of former ice lobes of the southernmost Patagonian Ice Sheet based on a glacial landsystems approach. J. Quat. Sci. 32 (6), 857–876. https://doi.org/10.1002/jqs.2890.

Darvill, C.M., Stokes, C.R., Bentley, M.J., Lovell, H., 2014. A glacial geomorphological map of the southernmost ice lobes of Patagonia: the Bahía Inútil – san Sebastián, magellan, Otway, skyring and Río gallegos lobes. J. Maps 10 (3), 500–520. https://doi.org/10.1080/17445647.2014.890134.

DaSilva, J.L., Anderson, J.B., Stravers, J., 1997. Seismic facies changes along a nearly continuous 24° latitudinal transect: the fjords of Chile and the northern Antarctic Peninsula. Marine Geology, COLDSEIS (seismic facies of glacigenic deposits) 143, 103–123. https://doi.org/10.1016/S0025-3227(97)00092-3.

Davies, B.J., Darvill, C.M., Lovell, H., Bendle, J.M., Dowdeswell, J.A., Fabel, D., García, J., Geiger, A., Glasser, N.F., Gheorghiu, D.M., Harrison, S., Hein, A.S., Kaplan, M.R., Martin, J.R.V., Mendelova, M., Palmer, A., Pelto, M., Rodés, Á., Sagredo, E.A., Smedley, R.K., Smellie, J.L., Thorndycraft, V.R., 2020. The evolution of the Patagonian Ice Sheet from 35 ka to the present day (PATICE). Earth Sci. Rev. 204, 103152. https://doi.org/10.1016/j.earscirev.2020.103152.

Davies, B.J., 2022. 4.13 - cryospheric geomorphology: dating glacial landforms II: radiometric techniques. In: Shroder, J.Jack F. (Ed.), Treatise on Geomorphology, second ed. Academic Press, Oxford, pp. 249–280.

De Muro, S., Tecchiato, S., Porta, M., Buosi, C., Ibba, A., 2018. Geomorphology of marine and glacio-lacustrine terraces and raised shorelines in the northern sector of Península Brunswick, Patagonia, Straits of Magellan, Chile. J. Maps 14 (2), 135–143. https://doi.org/10.1080/17445647.2018.1441759.

Dortch, J.M., Tomkins, M.D., Saha, S., Murari, M.K., Schoenbohm, L.M., Curl, D., 2022. A tool for the ages: the probabilistic cosmogenic age analysis Tool (P-caat). Quat. Geochronol. 71, 101323. https://doi.org/10.1016/j.quageo.2022.101323.

Evenson, E., P.A, B., Gosse, J., Baker, G., Jackofsky, D., Meglioli, A., I.W.D, D., Kraus, S., R, B.A., Berti, C., 2009. Enigmatic boulder trains, supraglacial rock avalanches, and the origin of "Darwin's boulders," Tierra del Fuego. GSA Today (Geol. Soc. Am.) 19 (12), 4–10. https://doi.org/10.1130/GSATG72A.1.

Fernández, R., Gulick, S., Rodrigo, C., Domack, E., Leventer, A., 2017. Seismic stratigraphy and glacial cycles in the inland passages of the Magallanes Region of Chile, southernmost South America. Mar. Geol. 386, 19–31. https://doi.org/10.1016/j.margeo.2017.02.006.

Fick, S.E., Hijmans, R.J., 2017. WorldClim 2: new 1-km spatial resolution climate surfaces for global land areas. Int. J. Climatol. 37 (12), 4302–4315. https://doi.org/10.1002/joc.5086.

Fontana, S.L., Bennett, K., 2012. Postglacial vegetation dynamics of western Tierra del Fuego. Holocene 22 (11), 1337–1350. https://doi.org/10.1177/0959683612444144.

García, J.-L., Hein, A.S., Binnie, S.A., Gómez, G.A., González, M.A., Dunai, T.J., 2018. The MIS 3 maximum of the Torres del Paine and Última Esperanza ice lobes in Patagonia and the pacing of southern mountain glaciation. Quat. Sci. Rev. 185, 9–26. https://doi.org/10.1016/j.quascirev.2018.01.013.

García, J.-L., Lüthgens, C., Vega, R.M., Rodés, Á., Hein, A., Binnie, S., 2021. A composite 10Be, IR-50 and 14C chronology of the pre-LGM full ice extent of the western Patagonian Ice Sheet in the Isla de Chiloé, south Chile (42°S). E&G - Quaternary Science Journal 70 (1), 105–128. https://doi.org/10.5194/egqsj-70-105-2021.

Garreaud, R., Lopez, P., Minvielle, M., Rojas, M., 2013. Large-scale control on the Patagonian climate. J. Climate 26 (1), 215–230. https://doi.org/10.1175/JCLI-D-12-00001.1.

Girault, I., Todisco, D., Çiner, A., Sarıkaya, M.A., Yıldırım, C., Quiquerez, A., Martin, F., Borrero, L., Fabel, D., Grandjean, P., Nehme, C., Mouralis, D., 2022. 10Be chronology of deglaciation and ice-dammed lake regression in the vicinity of the Mylodon Cave (Cerro Benítez, Patagonia, Chile). QSR 278, 107354. https://doi.org/10.1016/j.quascirev.2021.107354.

Glasser, N., Jansson, K., 2008. The glacial map of southern South America. J. Maps 4 (1), 175–196. https://doi.org/10.4113/jom.2008.1020.

Gowan, E.J., Zhang, X., Khosravi, S., Rovere, A., Stocchi, P., Hughes, A.L.C., Gyllencreutz, R., Mangerud, J., Svendsen, J.-I., Lohmann, G., 2021. A new global ice sheet reconstruction for the past 80 000 years. Nat. Commun. 12, 1199. https://doi.org/10.1038/s41467-021-21469-w.

Gurdiel, I., Rada, C., Malz, P., Braun, M., Casassa, G., 2022. Glacier inventory and recent variations of Santa Inés icefield, southern Patagonia. Arct. Antarct. Alp. Res. 54 (1), 202–220. https://doi.org/10.1080/15230430.2022.2071793.

Hagemann, J.R., Lamy, F., Arz, H.W., Lembke-Jene, L., Auderset, A., Harada, N., Ho, S.L., Iwasaki, S., Kaiser, J., Lange, C.B., Murayama, M., Nagashima, K., Nowaczyk, N., Martínez-García, A., Tiedemann, R., 2024. A Marine Record of Patagonian Ice Sheet Changes over the Past 140,000 Years, vol. 121. Proceedings of the National Academy of Sciences, e2302983121. https://doi.org/10.1073/pnas.2302983121.

Hall, B.L., Lowell, T.V., Bromley, G.R.M., Denton, G.H., Putnam, A.E., 2019. Holocene glacier fluctuations on the northern flank of Cordillera Darwin, southernmost South America. Quat. Sci. Rev. 222, 105904. https://doi.org/10.1016/j.quascirev.2019.105904.

Hall, B.L., Porter, C.T., Denton, G.H., Lowell, T.V., Bromley, G.R.M., 2013. Extensive recession of Cordillera Darwin glaciers in southernmost south America during

heinrich stadial 1. Quat. Sci. Rev. 62, 49–55. https://doi.org/10.1016/j.quascirev.2012.11.026.
Heaton, T.J., Köhler, P., Butzin, M., Bard, E., Reimer, R.W., Austin, W.E.N., Ramsey, C.B., Grootes, P.M., Hughen, K.A., Kromer, B., Reimer, P.J., Adkins, J., Burke, A., Cook, M. S., Olsen, J., Skinner, L.C., 2020. Marine20—the marine radiocarbon age calibration curve (0–55,000 cal BP). Radiocarbon 62, 779–820. https://doi.org/10.1017/RDC.2020.68.
Hein, A.S., Hulton, N.R.J., Dunai, T.J., Schnabel, C., Kaplan, M.R., Naylor, M., Xu, S., 2009. Middle Pleistocene glaciation in Patagonia dated by cosmogenic-nuclide measurements on outwash gravels. Earth Planet Sci. Lett. 286 (1–2), 184–197. https://doi.org/10.1016/j.epsl.2009.06.026.
Heusser, C.J., 1989a. Climate and chronology of Antarctica and adjacent South America over the past 30,000 yr. Palaeogeogr. Palaeocl. 76 (1–2), 31–37. https://doi.org/10.1016/0031-0182(89)90101-6.
Heusser, C.J., 1989b. Late Quaternary vegetation and climate of southern Tierra del Fuego. Quaternary Research 31, 396–406.
Heusser, C., 1998. Deglacial palaeoclimate of the American sector of the Southern Ocean. Late Glacial-Holocene records from the latitude of Canal Beagle (55oS), Argentine Tierra del Fuego. Palaeogeogr. Palaeocl. 141 (3–4), 277–301. https://doi.org/10.1016/S0031-0182(98)00053-4.
Heyman, J., Stroeven, A.P., Harbor, J.M., Caffee, M.W., 2011. Too young or too old: evaluating cosmogenic exposure dating based on an analysis of compiled boulder exposure ages. Earth Planet Sci. Lett. 302 (1–2), 71–80. https://doi.org/10.1016/j.epsl.2010.11.040.
Hodgson, D.A., Roberts, S.J., Izagirre, E., Perren, B.B., De Vleeschouwer, F., Davies, S.J., Bishop, T., McCulloch, R.D., Aravena, J.-C., 2023. Southern limit of the patagonian ice sheet. Quat. Sci. Rev. 321, 108346. https://doi.org/10.1016/j.quascirev.2023.108346.
Hogg, A.G., Heaton, T.J., Hua, Q., Palmer, J.G., Turney, C.S., Southon, J., Bayliss, A., Blackwell, P.G., Boswijk, G., Ramsey, C.B., Pearson, C., Petchey, F., Reimer, P., Reimer, R., Wacker, L., 2020. SHCal20 Southern Hemisphere calibration, 0–55,000 years cal BP. Radiocarbon 62 (4), 759–778. https://doi.org/10.1017/RDC.2020.59.
Holmlund, P., Fuenzalida, H., 1995. Anomalous glacier responses to 20th century climatic changes in Darwin Cordillera, southern Chile. J. Glaciol. 41 (139), 465–473. https://doi.org/10.3189/S0022143000034808.
Hughes, A.L.C., Gyllencreutz, R., Lohne, Ø.S., Mangerud, J., Svendsen, J.I., 2016. The last Eurasian ice sheets – a chronological database and time-slice reconstruction, DATED-1. Boreas 45, 1–45. https://doi.org/10.1111/bor.12142.
Jackofsky, D.S., Gosse, J.C., Cerling, T.E., Evenson, E.B., Klein, J., Easterbrook, D., Petersen, K.P., Spies, C., Sorenson, C.J., Caffee, M., 2000. Latitudinal Variations in the Timing of Alpine Glacier Retreat from LGM, Southern South America. Thirtieth Arctic Workshop, Boulder, Colorado.
Jowsey, P.C., 1966. An improved peat sampler. New Phytol. 65 (2), 245–248. https://doi.org/10.1111/j.1469-8137.1966.tb06356.x.
Kaiser, J., Lamy, F., Arz, H.W., Hebbeln, D., 2007. Dynamics of the millennial-scale sea surface temperature and Patagonian Ice Sheet fluctuations in southern Chile during the last 70 kyr (ODP Site 1233). Quaternary International, Lacustrine and marine archives of environmental variability across South America 161, 77–89. https://doi.org/10.1016/j.quaint.2006.10.024.
Kaplan, M.R., Coronato, A., Hulton, N.R.J., Rabassa, J.O., Kubik, P.W., Freeman, S.P.H.T., 2007. Cosmogenic nuclide measurements in southernmost South America and implications for landscape change. Geomorphology 87 (4), 284–301. https://doi.org/10.1016/j.geomorph.2006.10.005.
Kaplan, M.R., Fogwill, C.J., Sugden, D.E., Hulton, N.R.J., Kubik, P.W., Freeman, S.P.H.T., 2008. Southern patagonian glacial chronology for the last glacial period and implications for southern ocean climate. Quat. Sci. Rev. 27 (3–4), 284–294. https://doi.org/10.1016/j.quascirev.2007.09.013.
Kaplan, M.R., Strelin, J.A., Schaefer, J.M., Denton, G.H., Finkel, R.C., Schwartz, R., Putnam, A.E., Vandergoes, M.J., Goehring, B.M., Travis, S.G., 2011. In-situ cosmogenic 10Be production rate at Lago Argentino, Patagonia: implications for late-glacial climate chronology. Earth Planet Sci. Lett. 309 (1–2), 21–32. https://doi.org/10.1016/j.epsl.2011.06.018.
Kilian, R., Baeza, O., Breuer, S., Rios, F., Arz, H., Lamy, F., Wirtz, J., Baque, D., Korf, P., Kremer, K., Ríos, C., Mutschke, E., Simon, M., De Pol-Holz, R., Arevalo, M., Wörner, G., Schneider, C., Casassa, G., 2013. Late glacial and Holocene paleogeographical and paleoecological evolution of the Seno skyring and Otway fjord systems in the magellan region. An. Inst. Patagon. 41 (2), 5–26. https://doi.org/10.4067/S0718-686X2013000200001.
Kilian, R., Baeza, O., Steinke, T., Arevalo, M., Rios, C., Schneider, C., 2007a. Late Pleistocene to Holocene marine transgression and thermohaline control on sediment transport in the western Magellanes fjord system of Chile (53°S). Quat. Int. 161 (1), 90–107. https://doi.org/10.1016/j.quaint.2006.10.043.
Kilian, R., Schneider, C., Koch, J., Fesq-Martin, M., Biester, H., Casassa, G., Arévalo, M., Wendt, G., Baeza, O., Behrmann, J., 2007b. Palaeoecological constraints on late glacial and Holocene ice retreat in the southern Andes (53°S). Glob. Planet. Change 59 (1–4), 49–66. https://doi.org/10.1016/j.gloplacha.2006.11.034.
Lambeck, K., Rouby, H., Purcell, A., Sun, Y., Sambridge, M., 2014. Sea level and global ice volumes from the last glacial maximum to the Holocene. Proc. Natl. Acad. Sci. 111 (43), 15296–15303. https://doi.org/10.1073/pnas.1411762111.
Lambert, F., Bigler, M., Steffensen, J.P., Hutterli, M.A., Fischer, H., 2012. NOAA/WDS Paleoclimatology - EPICA Dome C Ice Core 800KYr Dust Flux Data at 25yr Resolution. NOAA National Centers for Environmental Information. https://doi.org/10.25921/yw3g-dm13. (Accessed 4 August 2023).
Lamy, F., Kilian, R., Arz, H.W., Francois, J.-P., Kaiser, J., Prange, M., Steinke, T., 2010. Holocene changes in the position and intensity of the southern westerly wind belt. Nature Geosci 3, 695–699. https://doi.org/10.1038/ngeo959.
Leger, T.P.M., Clark, C.D., Huynh, C., Jones, S., Ely, J.C., Bradley, S.L., Diemont, C., Hughes, A.L.C., 2024. A Greenland-wide empirical reconstruction of paleo ice sheet retreat informed by ice extent markers: PaleoGrIS version 1.0. Clim. Past 20, 701–755. https://doi.org/10.5194/cp-20-701-2024.
Lifton, N., Sato, T., Dunai, T.J., 2014. Scaling in situ cosmogenic nuclide production rates using analytical approximations to atmospheric cosmic-ray fluxes. Earth Planet Sci. Lett. 386, 149–160. https://doi.org/10.1016/j.epsl.2013.10.052.
Lira, M.-P., Garcia, J.-L., Bentley, M.J., Jamieson, S.S., Darvill, C.M., Hein, A., Fernández, H., Rodés, Á., 2022. The last glacial maximum and deglacial history of the Seno skyring ice lobe (52°S), southern Patagonia. Front. Earth Sci. https://doi.org/10.3389/feart.2022.892316.
Lisiecki, L.E., Raymo, M.E., 2005. A Pliocene-Pleistocene stack of 57 globally distributed benthic δ18O records. Paleoceanography 20 (1), PA1003. https://doi.org/10.1029/2004PA001071.
Lovell, H., Stokes, C.R., Bentley, M.J., Benn, D.I., 2012. Evidence for rapid ice flow and proglacial lake evolution around the central Strait of Magellan region, southernmost Patagonia. J. Quat. Sci. 27 (6), 625–638. https://doi.org/10.1002/jqs.2555.
Markgraf, V., Huber, U.M., 2010. Late and postglacial vegetation and fire history in southern Patagonia and Tierra del Fuego. Palaeogeogr. Palaeocl. 297 (2), 351–366. https://doi.org/10.1016/j.palaeo.2010.08.013.
McCoy, W.D., 1987. The precision of amino acid geochronology and paleothermometry. Quat. Sci. Rev. 6 (1), 43–54. https://doi.org/10.1016/0277-3791(87)90016-3.
McCulloch, R.D., Bentley, M.J., Tipping, R.M., Clapperton, C.M., 2005b. Evidence for late-glacial ice dammed lakes in the central Strait of magellan and Bahía Inútil, southernmost south America. Geogr. Ann. A. 87 (2), 335–362. https://doi.org/10.1111/j.0435-3676.2005.00262.x.
McCulloch, R.D., Bentley, M.J., 1998. Late glacial ice advances in the Strait of Magellan, southern Chile. Quat. Sci. Rev. 17 (8), 775–787. https://doi.org/10.1016/S0277-3791(97)00074-7.
McCulloch, R.D., Blaikie, J., Jacob, B., Mansilla, C.A., Morello, F., De Pol-Holz, R., San Román, M., Tisdall, E., Torres, J., 2020. Late glacial and Holocene climate variability, southernmost Patagonia. Quat. Sci. Rev. 229, 106131. https://doi.org/10.1016/j.quascirev.2019.106131.
McCulloch, R.D., Bentley, M.J., Fabel, D., Fernandez, H., Garcia, J.L., Hein, A., Huynh, C., Jamieson, S., Lira, M. Lüthgens, Nield, G., Roman, M., Tisdall, E.W., 2024. Solving the paradox of conflicting glacial chronologies: reconstructing the pattern of deglaciation of the Magellan cordilleran ice dome (53-54°S) during the Last glacial – interglacial transition. https://doi.org/10.1016/j.quascirev.2024.108866.
McCulloch, R.D., Fogwill, C.J., Sugden, D.E., Bentley, M.J., Kubik, P.W., 2005a. Chronology of the last glaciation in central Strait of magellan and Bahía Inútil, southernmost south America. Geogr. Ann. A. 87 (2), 289–312. https://doi.org/10.1111/j.0435-3676.2005.00260.x.
McCulloch, R.D., Mansilla, C.A., Morello, F., De Pol-Holz, R., San Román, M., Tisdall, E., Torres, J., 2019. Late glacial and Holocene landscape change and rapid climate and coastal impacts in the Canal Beagle, southernmost Patagonia. J. Quat. Sci. 34 (8), 674–684. https://doi.org/10.1002/jqs.3167.
Meglioli, A., 1992. Glacial geology and chronology of southernmost Patagonia and Tierra del Fuego, Argentina and Chile. Lehigh University, , PA, USA. Unpublished Ph.D. thesis.
Mendelova, M., Hein, A., Rhodes, A., Xu, S., 2020. Extensive mountain glaciation in central Patagonia during marine isotope stage 5. Quat. Sci. Rev. 227. https://doi.org/10.1016/j.quascirev.2019.105996.
Menounos, B., Clague, J.J., Osborn, G., Davis, P.T., Ponce, F., Goehring, B., Maurer, M., Rabassa, J., Coronato, A., Marr, R., 2013. Latest Pleistocene and Holocene glacier fluctuations in southernmost Tierra del Fuego, Argentina. Quat. Sci. Rev. 77, 70–79. https://doi.org/10.1016/j.quascirev.2013.07.008.
Mercer, J.H., 1976. Glacial history of southernmost South America. Quat. Res. 6 (2), 125–166. https://doi.org/10.1016/0033-5894(76)90047-8.
Miller, G.H., 1985. Aminostratigraphy of baffin island shell-bearing deposits. In: Andrews, J.T. (Ed.), Quaternary Environments, Baffin Island, Baffin Bay and West Greenland. Allen & Unwin, Winchester, MA, pp. 394–427.
Moreno, P.I., Lambert, F., Hernández, L., Villa-Martínez, R.P., 2023. Environmental evolution of western Tierra del Fuego (~54°S) since ice-free conditions and its zonal/hemispheric implications. Quat. Sci. Rev. 322, 108387. https://doi.org/10.1016/j.quascirev.2023.108387.
Moreno, P.I., Vilanova, I., Villa-Martínez, R., Dunbar, R.B., Mucciarone, D.A., Kaplan, M. R., Garreaud, R.D., Rojas, M., Moy, C.M., De Pol-Holz, R., Lambert, F., 2018. Onset and evolution of Southern Annular Mode-like changes at centennial timescale. Sci. Rep. 8, 3458. https://doi.org/10.1038/s41598-018-21836-6.
Pedro, J.B., Bostock, H.C., Bitz, C.M., He, F., Vandergoes, M.J., Steig, E.J., Chase, B.M., Krause, C.E., Rasmussen, S.O., Markle, B.R., Cortese, G., 2016. The spatial extent and dynamics of the Antarctic Cold Reversal. Nat. Geosci. 9 (1), 51–55. https://doi.org/10.1038/ngeo2580.
Peltier, C., Kaplan, M.R., Birkel, S.D., Soteres, R.L., Sagredo, E.A., Aravena, J.C., Araos, J., Moreno, P.I., Schwartz, R., Schaefer, J.M., 2021. The large MIS 4 and long MIS 2 glacier maxima on the southern tip of South America. Quat. Sci. Rev. 262, 106858. https://doi.org/10.1016/j.quascirev.2021.106858.
Porter, S.C., 1990. Character and ages of pleistocene drifts in a transect across the Strait of magellan. In: Rabassa, J. (Ed.), Quaternary of South America and Antarctic Peninsula. CRC Press, pp. 35–49.
Porter, S.C., Clapperton, C.M., Sugden, D.E., 1992. Chronology and dynamics of deglaciation along and near the Strait of Magellan, southernmost South America. Sveriges Geologiska Undersökning 81, 233–239.

Porter, S.C., Stuiver, M., Heusser, C.J., 1984. Holocene sea-Level changes along the Strait of magellan and Beagle Channel, southernmost south America. Quat. Res. 22 (1), 59–67. https://doi.org/10.1016/0033-5894(84)90006-1.

Prezzi, C.B., Orgeira, M.J., Coronato, A.M.J., Quiroga, D.R.A., Ponce, J.F., Núñez Demarco, P.A., Palermo, P., 2019. Geophysical methods applied to Quaternary studies in glacial environments: Río Valdez outcrop, Tierra del Fuego, Argentina. Quat. Int. 525, 114–125. https://doi.org/10.1016/j.quaint.2019.07.022.

Prieto, J., Winslow, M., 1994. El Cuatarnario del Estrecho de Magellanes I: sector Punta Arenas-Primera Angostura. An. Inst. Patagon. 21, 85–95.

Rabassa, J., Clapperton, C.M., 1990. Quaternary glaciations of the southern Andes. Quat. Sci. Rev. 9 (2–3), 153–174. https://doi.org/10.1016/0277-3791(90)90016-4.

Rabassa, J., Coronato, A., 2009. Glaciations in Patagonia and Tierra del Fuego during the Ensenadan Stage/Age (Early Pleistocene–earliest Middle Pleistocene). Quat. Int. 210 (1–2), 18–36. https://doi.org/10.1016/j.quaint.2009.06.019.

Rabassa, J., Coronato, A., Bujalesky, G., Salemme, M., Roig, C., Meglioli, A., Heusser, C., Gordillo, S., Roig, F., Borromei, A., Quattrocchio, M., 2000. Quaternary of Tierra del Fuego, southernmost South America: an updated review. Quat. Int., Nat Rutter Honorarium 68 (71), 217–240. https://doi.org/10.1016/S1040-6182(00)00046-X.

Rabassa, J., Coronato, A., Martínez, O., Reato, A., 2022. Last glacial maximum, late glacial and Holocene of Patagonia. In: Miotti, L., Salemme, M., Hermo, D. (Eds.), Archaeology of Piedra Museo Locality: an Open Window to the Early Population of Patagonia, the Latin American Studies Book Series. Springer International Publishing, Cham, pp. 59–84.

Rabassa, J., Heusser, C.J., Rutter, N., 1990. Late-glacial and Holocene of Tierra del Fuego, Argentina. In: Rabassa, J. (Ed.), Quaternary of South America and Antarctic Peninsula. CRC Press, pp. 327–351.

Rabassa, J., Coronato, A., Heusser, C.J., Roig Juñent, F., Borromei, A., Roig, C., Quattrocchio, M., 2006. The peatlands of Argentine Tierra del Fuego as a source for paleoclimatic and paleoenvironmental information. In: Martini, I.P., Martínez Cortizas, A., Chesworth, W. (Eds.), Developments in Earth Surface Processes, vol. 9. Elsevier, pp. 129–144. https://doi.org/10.1016/S0928-2025(06)09006-7.

Raedeke, L.D., 1978. Formas del terreno y depósitos cuaternarios : Tierra del Fuego central, Chile. Rev. Geol. Chile 5, 3–31.

Ramsey, C.B., 2009. Bayesian analysis of radiocarbon dates. Radiocarbon 51 (1), 337–360. https://doi.org/10.1017/S0033822200033865.

Reynhout, S.A., Kaplan, M.R., Sagredo, E.A., Aravena, J.C., Soteres, R.L., Schwartz, R., Schaefer, J.M., 2022. Holocene glacier history of northeastern Cordillera Darwin, southernmost South America (55°S). Quat. Res. 105, 166–181. https://doi.org/10.1017/qua.2021.45.

RGI 7.0 Consortium, 2023. Randolph Glacier Inventory - A Dataset of Global Glacier Outlines, Version 7.0. NSIDC: National Snow and Ice Data Center, Boulder, Colorado USA. https://doi.org/10.5067/f6jmovy5navz. :10.5067/f6jmovy5navz.

Rodriguez, P.C., Geiger, A.J., Ferri, L., Smedley, R.K., Garcia, J.-L., Herrera, G., 2023. Glacial geomorphology between the Gran Campo Nevado and Estrecho de Magallanes, Chile (52–53°S, 73°W). J. Maps 0, 1–14. https://doi.org/10.1080/17445647.2022.2153091.

Romero, M., Penprase, S.B., Van Wyk de Vries, M.S., Wickert, A.D., Jones, A.G., Marcott, S.A., Strelin, J.A., Martini, M.A., Rittenour, T.M., Brignone, G., Shapley, M. D., Ito, E., MacGregor, K.R., Caffee, M.W., 2024. Late quaternary glacial maxima in southern Patagonia: insights from the Lago Argentino glacier lobe. Clim. Past 1–33. https://doi.org/10.5194/cp-2024-24.

Sagredo, E.A., Moreno, P.I., Villa-Martínez, R., Kaplan, M.R., Kubik, P.W., Stern, C.R., 2011. Fluctuations of the Última Esperanza ice lobe (52°S), Chilean Patagonia, during the last glacial maximum and termination 1. Geomorphology 125 (1), 92–108. https://doi.org/10.1016/j.geomorph.2010.09.007.

Sanci, R., Orgeira, M.J., Coronato, A., Tófalo, R., Panarello, H.O., Quiroga, D., López, R., Palermo, P., Gogorza, C.S., 2021. Late Pleistocene glaciolacustrine MIS 3 record at Fagnano Lake, Central Tierra del Fuego, southern Argentina. Quat. Res. 102, 53–67. https://doi.org/10.1017/qua.2020.93.

Sandoval, F.B., De Pascale, G.P., 2020. Slip rates along the narrow magallanes Fault System, Tierra del Fuego region, Patagonia. Sci. Rep. 10, 8180. https://doi.org/10.1038/s41598-020-64750-6.

Schneider, C., Schnirch, M., Acuña, C., Casassa, G., Kilian, R., 2007. Glacier inventory of the gran Campo Nevado ice cap in the southern Andes and glacier changes observed during recent decades. Global Planet. Change 59 (1–4), 87–100. https://doi.org/10.1016/j.gloplacha.2006.11.023.

Soteres, R.L., Peltier, C., Kaplan, M.R., Sagredo, E.A., 2020. Glacial geomorphology of the Strait of magellan ice lobe, southernmost Patagonia, south America. J. Maps 16 (2), 299–312. https://doi.org/10.1080/17445647.2020.1736197.

Stern, C., Henríquez, W., Villa-Martínez, R., Sagredo, E., Aravena, J., De Pol-Holz, R., 2016. Holocene tephrochronology around Cochrane (~47° S), southern Chile. Andean Geol. 43, 1–19. https://doi.org/10.5027/andgeoV43n1-a01.

Sugden, D.E., Hulton, N.R.J., Purves, R.S., 2002. Modelling the inception of the Patagonian icesheet. Quaternary International, Inception: Mechanisms, patterns and timing of ice sheet inception 95–96 55–64. https://doi.org/10.1016/S1040-6182(02)00027-7.

Sugden, D.E., Bentley, M.J., Fogwill, C.J., Hulton, N.R.J., McCulloch, R.D., Purves, R.S., 2005. Late-glacial glacier events in southernmost South America: a blend of 'Northern' and 'Southern' hemispheric climatic signals? Geogr. Ann. A. 87 (2), 273–288. https://doi.org/10.1111/j.0435-3676.2005.00259.x.

Uribe, P., 1982. Deglaciacion en el sector central del Estrecho de Magallanes: consideraciones geomorfologicos y cronologica. An. Inst. Patagonia 13, 103–111.

Vanneste, H., De Vleeschouwer, F., Martínez-Cortizas, A., Scheffer, C., Piotrowska, N., Coronato, A., Le Rouz, G., 2015. Late-glacial elevated dust deposition linked to westerly wind shifts in southern South America. Sci. Rep. 5, 11670. https://doi.org/10.1038/srep11670.

Waldmann, N., Ariztegui, D., Anselmetti, F.S., Coronato, A., Austin, J.A., 2010. Geophysical evidence of multiple glacier advances in Lago Fagnano (54°S), southernmost Patagonia. Quat. Sci. Rev. 29 (9–10), 1188–1200. https://doi.org/10.1016/j.quascirev.2010.01.016.